©Verein zur Förderung der Paläontologie am Institut für Paläontologie, Geozentrum Wien

Beitr. Paläont., **19**:191–217, Wien 1994

Facies and palaeoecology of rhodoliths and acervulinid macroids in the Eocene of the Krappfeld (Austria)

Fazies und Paläoökologie von Rhodolithen und acervuliniden Macroiden im Eozän des Krappfeldes (Österreich)

by

Michael RASSER*

RASSER, M., 1994. Facies and palaeoecology of rhodoliths and acervulinid macroids in the Eocene of the Krappfeld (Austria). — Beitr. Paläont., **19**:191–217, 6 Figures, 1 Table, 4 Plates, Wien.

Contents

Abstract

The Eocene of the Krappfeld represents the latest marine deposits in the basin of the Central Alpine Krappfeld Gosau. Topmost (Ypresian/Lutetian) sediments represent limestones with accumulations of coralline algae and acervulinid foraminifera.

Two rhodolith accumulations and one acervulinid macroid accumulation can be distinguished. Each accumulation is characterized by distinct growth forms, nuclei and taxonomic compositions of the nodules.

The dominant rhodolith builder is *Sporolithon*. Columnar growth forms (showing short stubby protuberances) are more frequent than laminar and branched forms. The nuclei consist of corals or tests of *Nummulites*. Acervulinid macroids are dominated by *Acervulina* (= *Solenomeris*) *ogormani*. Large columnar growth forms without preserved nuclei and small laminar macroids with coral nuclei occur.

Using the taxonomic composition and growth form of rhodoliths and macroids the sedimentary environment can be reconstructed.

* Institut für Paläontologie der Universität Wien, Universitätsstraße 7/II, A-1010 Vienna, Austria

Zusammenfassung

Das Eozän des Krappfeldes repräsentiert die jüngsten marinen Sedimente im Becken der zentralalpinen Gosau. Das Hangendste (Ypresium/Lutetium) besteht aus Kalken mit Akkumulationen von Rhodolithen und Macroiden aus acervuliniden Foraminiferen.

Zwei Rodolith- und eine Macroid-Akkumulation können definiert werden. Diese unterscheiden sich durch Wuchsformen, Kerne und taxonomische Zusammensetzungen. Die Rhodolithen bestehen vorwiegend aus *Sporolithon* und weisen vor allem columnare, weniger häufig laminare oder verzweigte Wuchsformen auf. Als Kern dienen vor allem Korallen und Nummuliten. Macroide bestehen vorwiegend aus der inkrustierenden Foraminifere *Acervulina (=Solenomeris) ogormani*. Diese bildet große columnare Macroide ohne erhaltenen Kern und kleine laminare mit Kernen aus Korallenfragmenten.

Die Analyse der taxonomischen Zusammensetzungen und Wuchsformen von Rhodolithen und Macroiden ermöglichen eine Rekonstruktion des Ablagerungsraumes.

1. Introduction

Coralline algae (Corallinaceae, Rhodophyta) are frequent carbonate producers in the Cenozoic. In the Eastern Alps, occurrences of Paleogene coralline algae are restricted to small relic areas (MOUSSAVIAN, 1984). Compared to the Neogene, Paleogene coralline algae are less diverse on the specific level. However, the variability of growth forms points to adaptations to quite different environments. An understanding of Paleogene palaeogeography and facies requires a detailed taxonomic and palaeoecological documentation.

Nongeniculate crustose coralline algae predominantly encrust hard substrate and are able to form unattached rhodoliths in response to unstable substrate. A review of rhodoliths is given in BOSENCE (1991). The important role of acervulinid foraminifera as frame builders in the Paleogene was recently pointed out by PERRIN (1992)

©Verein zur Förderung der Paläontologie am Institut für Paläontologie, Geozentrum Wien

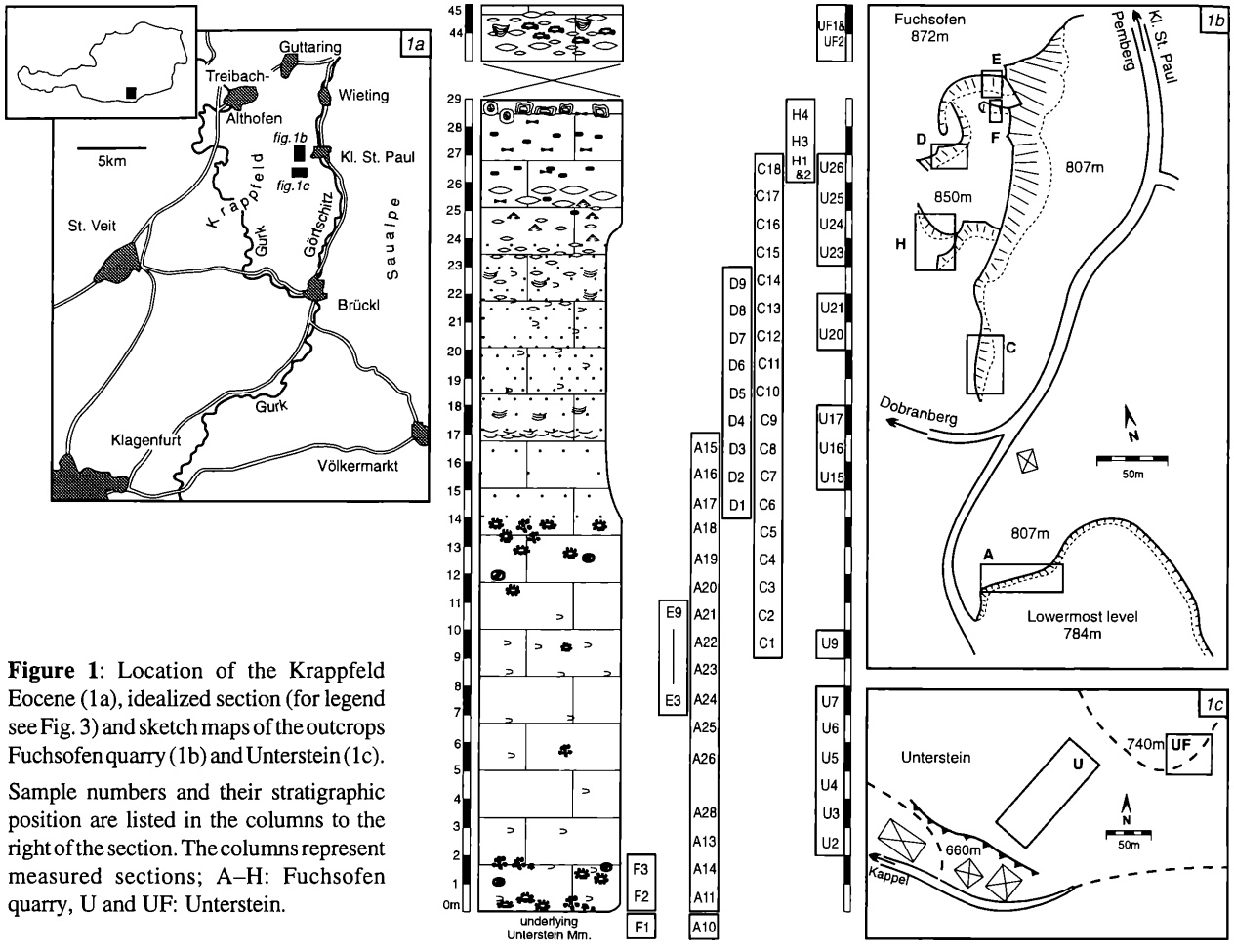

Figure 1: Location of the Krappfeld Eocene (1a), idealized section (for legend see Fig. 3) and sketch maps of the outcrops Fuchsofen quarry (1b) and Unterstein (1c).

Sample numbers and their stratigraphic position are listed in the columns to the right of the section. The columns represent measured sections; A–H: Fuchsofen quarry, U and UF: Unterstein.

and PLAZIAT & PERRIN (1992). They are analogous to coralline algae in their encrusting habit and ability to form unattached aggregates (macroids: HOTTINGER, 1983). In the Eocene of the Krappfeld Gosau, both organism groups are represented in the form of rhodoliths and macroids. Taxonomic composition, internal structure and growth form depend on the ecological conditions of the environment. Consequently, these features – combined with an analysis of the sedimentary facies – provide a great potential for the reconstruction of environments.

The aim of this study is (1) to document the rhodolith- and macroid-forming organisms of the study area and their relation to the sedimentary facies, (2) to quantify overgrowth within the rhodoliths/macroids in terms of frequency and (3) to reconstruct the paleoecological conditions using the encrusting organisms.

2. Study area

The Krappfeld is situated on the eastern margin of the Gurktal Nappe, belonging to the Upper Austroalpine Unit (TOLLMANN, 1977). The eastern margin of this unit is the Görtschitz fault, which is responsible for the complicated outcrop situation of the study area.

The Eocene of the Krappfeld represents the final deposits of an intraalpine Gosau basin. Gosau basins, induced by the Alpidic evolution of the Eastern Alps (FAUPL et al., 1987), are delimited to the Upper Austroalpine Unit. The Gosau development in the Eastern Alps contains different sedimentary environments from Upper Cretaceous to Upper Eocene. In the Paleogene of the Northern Calcareous Alps, turbiditic sediments in the north contrast with a belt of shallow water carbonates in the south.

The basin of the Central Alpine Krappfeld Gosau is an exception as it includes Paleogene sediments outside the Northern Calcareous Alps. The Eocene occurrence is very small-scaled and highly isolated. After a hiatus above Cretaceous turbidites, Paleogene sediments start in the Ilerdian with continental sediments (coal-bearing clays) reaching up to the Lower Ypresian. The marine transgression begins with nummulitic marls, followed by pure nummulitic limestones (HINTE, 1963; WILKENS, 1989, 1991). The latter are overlain by the Ypresian/Lutetian study section including coralline algal limestones (compare Fig. 2).

The two best outcrops (Fig. 1) were studied. One is the location "Unterstein" (Fig. 1c), SW Kl. St. Paul, where the longest, but poorly outcropped, section is available. It is a reference section for the partial sections of the more important location "Fuchsofen quarry" (Fig. 1b).

©Verein zur Förderung der Paläontologie am Institut für Paläontologie, Geozentrum Wien

3. Methods

Paleogene and Neogene tectonic faults (GOSEN, 1989) caused a complicated outcrop situation and required a correlation of 8 partial sections. Parallelisation of sections was carried out by microfacies analysis, as weathered surfaces provide rather poor outcrops. Samples were taken in a vertical distance of one meter. Partial sections, sample numbers and their positions in the outcrops are presented in Fig. 1.

150 thin sections (50 x 50 mm) and several polished slabs where prepared. For microfacies analysis, the following 30 samples where considered: A11–A18, C6–C17, H1, H3, H4, and UF3 (Fig. 3). One thin section of each sample was analysed. Several comparison charts (e.g. BACCELLE & BOSELLINI, 1965) were used to determine sedimentary textures and the quantitative distribution of components. The limestone classification is according to DUNHAM (1962), extended by EMBRY & KLOVAN (1972).

The abundance of rhodoliths and their growth forms were estimated in the field and on polished slabs; they are not, however, considered in the "sedimentary textures" and microfacies analysis (Fig. 3). Also, the bivalves of the Siliciclastic *Pseudogypsina* Facies and the oysters of the *Nummulites*–Rhodolith Facies are not considered quantitatively.

The composition of encrusting communities within rhodoliths/macroids and the abundance of overgrowths where analysed by putting a grid (drawn on a transparent foil) with a cell size of 4 mm2 over the thin section. The frequency of species was estimated for each cell. In the same manner, the frequency and sequence of overgrowths was counted and documented in 3–dimensional charts (Fig. 4). Intraspecific overgrowths and crust thickness were not considered. Therefore one species forming thin crusts may have a low frequency but a high percentage of overgrowths.

4. Lithostratigraphy

The first lithostratigraphic subdivision of the Krappfeld Paleogene was introduced by PENECKE (1884); this has been renewed by HINTE (1963). Recently the Krappfeld Paleogene was studied by WILKENS (1989), who introduced a new lithostratigraphic concept. The latter has been revised again by WILKENS (1991) (Fig. 2).

5. Study section

The study section can easily be separated from the underlying nummulitid-alveolinid limestones (compare Fig. 2) by its encrusting organisms (coralline algae, acervulinid foraminifera) and quartz content. The occurrence of the foraminifera *Acervulina ogormani, A. linearis* and *Pseudogypsina multiformis* put both lithostratigraphic members into the Ypresian – Lutetian (WILKENS, 1989; according to MOUSSAVIAN, 1984).

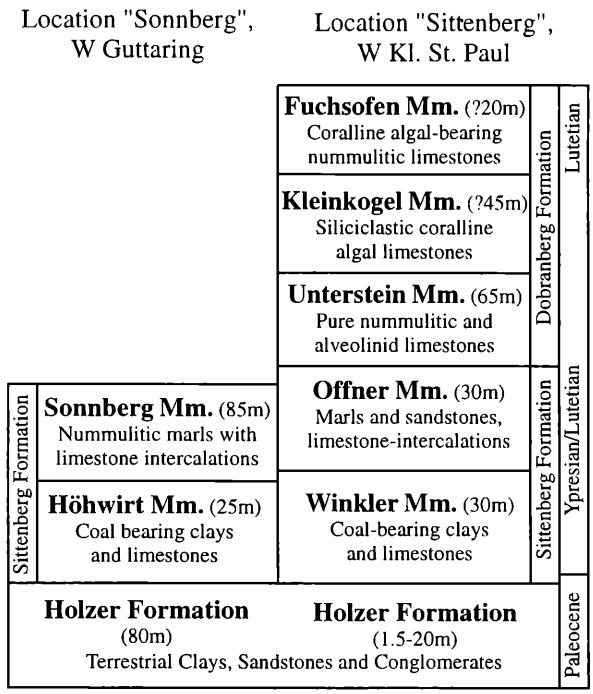

Figure 2: Lithostratigraphy of the Krappfeld Paleogene after WILKENS (1991). Study section contains Kleinkogel and Fuchsofen Member.

The study section starts with a pack- to grainstone containing rhodoliths in rock-forming quantities (Fig. 3). Rhodoliths are predominantly columnar and mainly formed by *Sporolithon* sp. A. Other major components include U-shaped tests of *Pseudogypsina multiformis*, fragments of coralline algae and other foraminifera. The muddy matrix is not distributed regularly; in thin section, pure biomicrite is located close to biosparite. This rhodolith limestone (not more than 2 m thick) is summarized into the Rhodolith – *Pseudogypsina* Facies and represented in two partial sections (A and F).

Upward, rhodoliths and muddy matrix become less frequent, but the composition of the main components remains the same; *P. multiformis* (often > 1 mm) characterizes the microfacies. Its dominance (39 % of the main components) causes an increasing mean grain size to a peak of 710 µm (rhodoliths are not considered). They are often coated by micrite envelopes, especially in partial section A. Additionally, the sorting of components is very good at this maximum. Other larger foraminifera are rare, except *Nummulites* div. spec. which constitutes up to 12 % of the foraminifera. Rhodoliths only occur in several small accumulations.

Upsection, *P. multiformis* decreases rapidly together with an increasing abundance of coralline algal fragments and foraminifera. The absence of *P. multiformis*, muddy matrix and terrigenous components characterizes this grain- to floatstone. Rhodoliths are again rock-forming.

©Verein zur Förderung der Paläontologie am Institut für Paläontologie, Geozentrum Wien

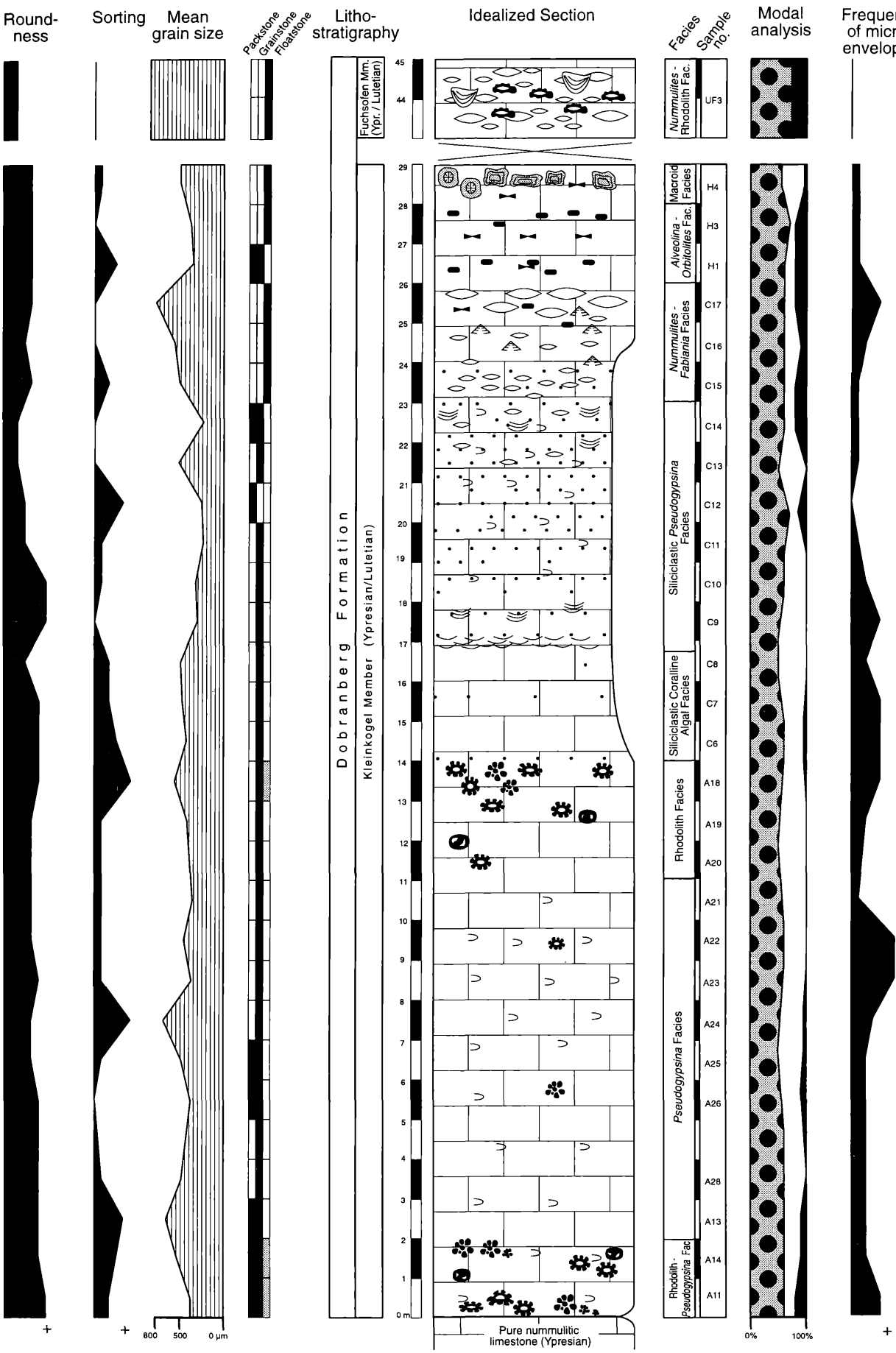

©Verein zur Förderung der Paläontologie am Institut für Paläontologie, Geozentrum Wien

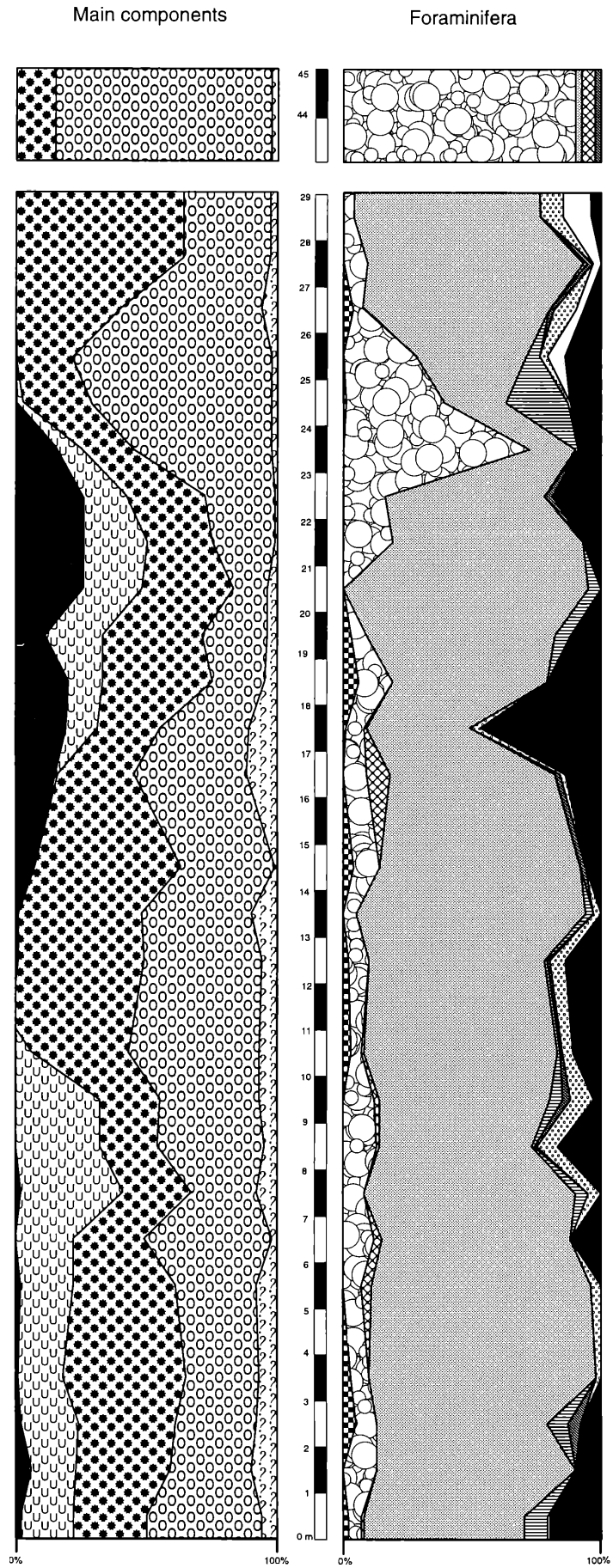

LEGEND - IDEALIZED SECTION

- Limestone
- Terrigenous limestone
- *Pseudogypsina multiformis*
- *Nummulites* div. spec.
- *Alveolina* div. spec.
- *Orbitolites* sp. indet.
- *Fabiania cassis*
- *Ostrea* sp. indet.
- Lumachelle
- Columnar rhodolith
- Laminar rhodolith
- Branched rhodolith
- Acervulinid macroid with coral-nucleus
- Acervulinid macroid
- Rhodolith with *Nummulites* - nucleus

LEGEND - MODAL ANALYSIS

- Particles
- Sparry cement
- Micrite

LEGEND - MAIN COMPONENTS

- Quartz
- *Pseudogypsina multiformis*
- Coralline algal fragments
- Foraminifera
- Not classified

LEGEND - FORAMINIFERA

- Smaller agglutinated foraminifera
- Nummulitidae
- *Discocyclina* sp. indet.
- Other rotaliid foraminifera
- *Fabiania cassis*
- *Sphaerogypsina globulus*
- *Alveolina* div. spec.
- *Orbitolites* sp. indet.
- Smaller miliolid foraminifera

Figure 3: Lithology and microfacies of the study section.

For abundancy of rhodoliths, acervulinid macroids and molluscs see symbols in the section; note that they are not included in the main components and sedimentary textures.

Sample numbers represent thin sections used for microfacies analysis. Their positions in the partial sections are listed in Fig. 1.

©Verein zur Förderung der Paläontologie am Institut für Paläontologie, Geozentrum Wien

Their growth forms are the same as at the base of the section, but the acervulinid foraminifer *Acervulina ogormani* occurs for the first time. A coarsening upward of coralline algal and rotaliid foraminiferal fragments leads to an increasing mean grain size of non-rhodolith components (up to 580 µm). Fragments of rotaliid foraminifera are mostly coated by micrite envelopes. This Rhodolith Facies is well developed in section A, which provides the samples used for microfacies analysis. In partial section C this facies is lacking, rhodoliths are rare and *P. multiformis* is still rock-forming. There is no outcrop in the U-section (see Fig. 1).

Rhodoliths of the above-described section are combined to the Lower Rhodolith Accumulation. Although the facies are different, rhodoliths show corresponding growth forms, nuclei and, partially, taxonomic composition.

An increasing importance of quartz along with an absence of rhodoliths and macroids characterize the overlying part of the section.

The terrigenous limestones start with grainstones dominated by coralline algal fragments, foraminifera and quartz (up to 15 %) but lacking *P. multiformis* and macrofossils. This facies (Siliciclastic Coralline Algal Facies) only occurs in the partial sections A and D. Section C (samples C6–8) shows a direct transition from the *P. multiformis* Facies to the overlying facies. In U-section, the first sample (U15) after a gap contains tests of *P. multiformis* and thus passes over to the overlying facies. A distinct lumachelle bed leads over to a terrigenous pack- to grainstone characterized by several univalved shell accumulations (Siliciclastic *Pseudogypsina* Facies). The lumachelle bed serves as a marker horizon and allows a correlation of the partial sections A, D and C. Section U lacks this lumachelle (perhaps due to the poor outcrop situation). Together with an increasing concentration of quartz grains (up to 26 % of the main components), *P. multiformis* (up to 25 %) and *Nummulites* (20 % of the foraminifera, less frequent in the U-section) become abundant. Contrary to the *Pseudogypsina* Facies, *P. multiformis* tests are not coated by micrite envelopes. Smaller miliolid foraminifera show their maximum here. Above this sequence with shell accumulations, quartz and *P. multiformis* decrease rapidly and disappear; coralline algal fragments reach their minimum of the section. They are replaced by other foraminifera: *Nummulites* div. spec. (up to 72 % of the foraminifera) and unfragmented tests of *Fabiania cassis* with up to 24 % (*Nummulites–Fabiania* facies) are abundant. The high percentage of coated foraminifera causes a high abundance of micrite envelopes. *Nummulites* tests in partial section C are imbricated and coarsen upward (up to 20 mm), causing a maximum of the mean grain size (800 µm). *Nummulites* are less frequent in the U-section and lack imbrications. In both sections, *Alveolina* div. spec. become abundant and *Orbitolites* sp. indet. appears for the first time.

These larger miliolid foraminifera mark the transition to a packstone (and floatstone with packstone matrix) with quite different facies (*Alveolina–Orbitolites* facies). The percentage of muddy matrix is partially higher than in the underlying facies. Generally the frequency of foraminifera decreases from 75 to 34 % of the main components, whereas coralline algal fragments distinctively increase to 64 %. The facies is best developed in the H-section. Partial section C only contains the base of this facies, as it is cut tectonically. In the U-section, the *Alveolina - Orbitolites* facies is absent. Instead, small macroids with well preserved coral nuclei are significant (U26).

Upward, the frequency of muddy matrix distinctly decreases and the first acervulinid macroids occur in rock-forming quantities. They mark the "Macroid Facies" (only outcropped in section H), characterized by large columnar macroids (up to 10 cm). This accumulation is not more than 2m thick and cut by a tectonic fault. Larger miliolid foraminifera (*Alveolina* div. spec. and *Orbitolites* sp. indet.) are still characteristic.

The section of the outcrop Fuchsofen ends here. No outcrop of the "Nummulitidae Faziesassoziationen" after WILKENS (1991) could be found (except for some pebbles). Only at the outcrop Unterstein (section UF) could a corresponding facies be found after a gap of 15 m. This gap is partially caused by tectonic faults and thus the distance is an estimation.

This topmost part is a rhodolith-bearing pure packstone, absolutely dominated by *Nummulites* div. spec. (54 % of the main components) with varying test size (up to 8 cm). A majority of the tests is encrusted by coralline algae, forming columnar rhodoliths. Micrite envelopes are lacking and the mean grain size is the highest of the whole section (870 µm). The macrofauna is characterized by large oysters (which are not considered in the distribution of the main components in Fig. 3).

This facies seems to contain the final marine sediments of the Krappfeld Gosau basin which are overlain by Miocene fluvial sediments. According to WILKENS (1991), several fluvial pebbles of the Krappfeld could be of Upper Eocene age.

6. Facies

6.1. Rhodolith – *Pseudogypsina* Facies

Only two meters thick pack- to grainstone. Components:sparry cement:micrite (C:S:M) = 60:20:20% at the base, 60:30:10 at the top. Rhodoliths (basal horizon of the Lower Rhodolith Accumulation) are rock-forming, dominated by *Sporolithon* sp. A; growth forms are predominantly ellipsoidal and columnar, no acervulinid macroids occur. Main components (rhodoliths not considered) dominated by foraminifera (45–31 %), coralline algal fragments (28–36 %) and *Pseudogypsina multiformis* (17–20 %). Terrigenous components (mainly moderately to well-sorted quartz) do not exceed 5 %. Foraminifera: predominantly unidentified rotaliid foraminifera (62–77 %), smaller miliolid foraminifera (20–10

©Verein zur Förderung der Paläontologie am Institut für Paläontologie, Geozentrum Wien

%), *Nummulites* div. spec. (6–13 %), and *Fabiania cassis* (0–9 %). Characteristically, corals in all facies are preserved as rhodolith- and macroid-nuclei only. Mean grain size (rhodoliths not included): 400–550 µm. Samples: A11, A14 (see Fig. 3).

6.2. *Pseudogypsina* Facies

Differs from the underlying facies predominantly by the lower frequency of rhodoliths. About 9 m thick grain- to packstone, C:S:M(%) = 60:30:10 at the base, but mostly 60:40:0. Rhodoliths (Lower Rhodolith Accumulation) less frequent, no acervulinid macroids. Main components (rhodoliths not considered) are coralline algal fragments (22–47 %), foraminifera (25–50 %) and *P. multiformis* (17–39 %). Quartz is rare to lacking. Foraminifera: unidentified rotaliid foraminifera (59–88 %) are dominant. *Fabiania cassis* occurs again alongside *Alveolina* div. spec., *Sphaerogypsina globulus* and *Discocyclina* sp. indet.; Foraminifera never exceed 5 %. *Nummulites* div. spec.: 4–13 % of the foraminifera. Mean grain size: 370–710 µm. Samples: A13, A28, A26, A25, A24, A23, A22, A21.

6.3. Rhodolith Facies

Max. 3 m thick grainstone and floatstone with grainstone matrix. C:S:M(%) = 50:50:0. Rhodoliths (upper horizon of the Lower Rhodolith Accumulation) are rock-forming; they correspond with both facies below. Main components (except rhodoliths) are coralline algal fragments (46 %) and foraminifera (42–45 %). *P. multiformis* is lacking, as muddy matrix and quartz. The distribution of other larger foraminifera corresponds to the facies below. Mean grain size: 430–580 µm. The grainstones are poorly to well sorted. Micrite envelopes are frequent. Samples: A18–A20.

6.4. Siliciclastic Coralline Algal Facies

Max. 3 m thick terrigenous grainstone. C:S:M(%) = 60:35:5 – 50:50:0. No rhodoliths. The main components are coralline algal fragments (29–56 %) and foraminifera (36–43 %). Quartz becomes frequent, with 7 % at the base and 15 % in the upper part. *P. multiformis* is lacking (except a few specimens in the uppermost part). Foraminifera: unidentified rotaliid foraminifera decrease from 78 to 46 %, smaller miliolid foraminifera increase from 6 to 14 %. *Discocyclina*. sp. indet.: 0–9 %. Mean grain size: 440–500 µm. Moderate sorting and roundness, micrite envelopes are abundant. Samples: C6–C8.

6.5. Siliciclastic *Pseudogypsina* Facies

About 6 m thick terrigenous pack- to grainstone. C:S:M(%) = 50:50:0 – 70:15:15. No rhodoliths and acervulinid macroids occur. Main components (shell accumulations not included): coralline algal fragments (24–42 %), foraminifera (13–34 %), quartz (11–26 %), and *P. multiformis* (12–25 %). Foraminifera are dominated by unidentified rotaliid foraminifera (40–95 %), smaller miliolid foraminifera (0–47 %) and *Nummulites* div. spec. (0–30 %). Mean grain size: 240–530 µm. Very poorly to well sorted, frequency of micrite envelopes decreases upward. Samples: C9–C14.

6.6. *Nummulites – Fabiania* Facies

Floatstone with pack- to grainstone matrix, about 3 m thick. C:S:M(%) = 60:30:10 – 60:20:20. No rhodoliths or acervulinid macroids. Main components are foraminifera (52–75 %) and coralline algae (20–24 %). Both quartz (18–0 %) and *P. multiformis* (10–0 %) decrease rapidly. Foraminifera: *Nummulites* div. spec.: 28–72 %, Ø 5–20 mm. Unfragmented tests of *Fabiania cassis*: max. 24 %. Unidentified rotaliid foraminifera: 18–41 %. *Orbitolites* sp. indet.: max. 7 %, *Alveolina* div. spec.: max. 3 %. Mean grain size: 520–802 µm (because of the large *Nummulites* tests). Sorting is poor to moderate. Samples: C15–C17.

6.7. *Alveolina – Orbitolites* Facies

Pack- to grain- and floatstone. C:S:M(%) = 60:20:20 – 70:10:20. No rhodoliths. Main components: coralline algae (increasing from 40 to 64 %) and foraminifera (decreasing from 55 to 34 %). Quartz and *P. multiformis* are absent. Characteristic foraminiferal association: *Alveolina* div. spec. (up to 10 %) and *Orbitolites* sp. indet. (never exceeding 3 %). Unidentified rotaliid foraminifera: 72–85 %. Mean grain size: 360–380 µm, poor to well sorted. Micrite envelopes are not frequent. Samples: H1, H3.

6.8. Macroid Facies

Grainstone to floatstone with grainstone matrix. C:S:M(%) = 55:40:5. Acervulinid macroids (dominated by *Acervulina ogormani*) are rock-forming (Ø up to 10 cm), no rhodoliths. Main components (except macroids) are similar to the *Alveolina – Orbitolites* facies. Foraminifera: unidentified rotaliid foraminifera: 72 %, *Orbitolites* sp. indet.: 12 %. Neither *Alveolina* div. spec. nor *Nummulites* div. spec. exceed 10 %. Mean grain size: 510 µm, poor sorting, micrite envelopes are not frequent. Sample: H4.

6.9. *Nummulites* – Rhodolith Facies

Floatstone with packstone matrix. C:S:M(%) = 70:0:30. Columnar rhodoliths, characterized by *Nummulites* nuclei. Main components (oysters are not considered) are foraminifera with 83 % and coralline algal fragments with only 15 %. Foraminifera are dominated by tests of *Nummulites*

©Verein zur Förderung der Paläontologie am Institut für Paläontologie, Geozentrum Wien

div. spec. (91 %) and their fragments. Differs from the *Nummulites–Fabiania* facies in the higher percentage of nummulites, their thicker tests and the lack of sparry cement. Mean grain size: 870 µm. Sorting is very poor and there are no micrite envelopes. Sample: UF1.

7. Taxonomy

Class Rhodophyceae RABENHORST, 1863
Order Corallinales SILVA & JOHANSEN, 1986
Family Corallinaceae LAMOUROUX, 1812

Terminology according to the revision of WOELKERLING (1988) using "core filaments" instead of "hypothallus", and "peripheral filaments" instead of "perithallus"

Genus *Lithoporella*(FOSLIE) FOSLIE, 1909

Dimerous thallus, lacking protuberances.

Lithoporella melobesioides (FOSLIE) FOSLIE, 1909
(Pl. 3, Fig. 3)

1904 *Mastophora (Lithoporella) melobesioides* FOSLIE–WEBER VAN BOSSE & FOSLIE, pp. 73–77, Text-Figs. 30–32.
1983c *Lithoporella melobesioides* (FOSLIE) FOSLIE–BOSENCE, pp. 165–166, Pl. 18, Fig. 1.

Thallus morphology: crustose thallus, partially growing unattached.
Anatomy can easily be recognized by its unistratose cell layers (predominantly not more than two consecutive layers) composed of large cells. Cell length = 9–16 µm (mean (M) = 14, standard deviation (SD) = 2.5); cell diameter = 6–16 µm (M = 10, SD = 2.2); ratio length/diameter = 0.9–2.5 (M = 1.4, SD = 0.4, number of measured cells (N) = 20).
Sporangia: rare; height = 78–126 µm (M = 104, SD = 20.3); diameter = 40–60 µm (M = 50, SD = 8.3); ratio height/diameter = 1.9–2.4 (M = 2.1, SD = 0.3, N = 4).
Occurrence: in rhodoliths and macroids of the whole section, but never frequent.

Genus *Lithothamnion* HEYDRICH, 1897

Former name: *Lithothamnium* PHILIPPI, 1837. Thallus monomerous and plumose.

Lithothamnion sp.
(Pl. 3, Figs. 4, 5; Pl. 2, Fig. 6)

Thallus morphology: growth form predominantly protuberant, partially growing unattached.
Anatomy thallus predominantly composed of thin crusts (200–300 µm). Core filaments well developed and regular. Some derivates of the branched core filaments curve outward, some curve toward the substrate. The core is 88–100 µm thick. Cell length = 12–22 µm (M = 16, SD = 2.9); cell diameter = 7–10 µm (M = 8, SD = 1); ratio cell length/diameter = 1.2–3.1 (M = 1.9, SD = 0.5, N = 15). Cell length of peripheral filaments = 8–13 µm (M = 12, SD = 1.8); cell diameter = 7–12 µm (M = 10, SD = 1.5); ratio cell length/diameter = 0.7–1.9 (M = 1.3, SD = 0.3, N = 20).
Sporangia: multiporate conceptacles, restricted to (mostly small) protuberances; height = 174–195 µm (M = 182, SD = 10.1); diameter = 295–420 µm (M = 341, SD = 51.5); ratio height/diameter = 0.5–0.6 (M = 0.5, SD = 0.1, N = 5).
Occurrence: only a few occurrences in rhodoliths of the basal horizon of the Lower Rhodolith Accumulation and in the Upper Rhodolith Accumulation.

Genus *Sporolithon* HEYDRICH, 1897

Former name: *Archaeolithothamnium* ROTHPLETZ, 1891. Thallus monomerous and plumose. Sporangia are small and usually aligned in tiers; persistent groups of calcified filaments are interspersed between the sporangia.

Sporolithon sp. A
(Pl. 2, Figs. 1, 2, 3, 6, 7; Pl. 3, Fig. 1)

Thallus morphology: protuberant, less frequently crustose. Only the protuberances (mean diameter 1.2 mm, mean height 2 mm) contain sporangia. Forming monospecific rhodoliths.
Anatomy some derivates of the branched core filaments curve outward, but they never curve toward the substrate. Core thickness mostly 100 µm. Cells rather small and rarely well developed. Cell length of core filaments = 10–32 µm (M = 19, SD = 6.1); cell diameter = 9–14 µm (M = 11, SD = 1.4); ratio cell length/diameter = 0.9–3.6 (M = 1.8, SD = 0.7, N = 20). Cell length of peripheral filaments = 13–22 µm (M = 17, SD = 2.1); cell diameter = 10–15 µm (M = 12, SD = 1.6); ratio cell length/diameter = 0.9–1.7 (M = 1.4, SD = 0.2, N = 20).
Sporangia: very regular rows with up to 25 ovate conceptacles. Up to six filaments can be interspersed between the sporangia, but they also may join together. The filament walls either curve outward to make place for a sporangium so that it is constructed within one filament, or several filaments end below the sporangia. Height of sporangia = 68–84 µm (M = 75, SD = 5.4); diameter = 36–49 µm (M = 42, SD = 4.1); ratio height/diameter = 1.5–2.1 (M = 1.8, SD = 0.2, N = 20).
Occurrence: dominant rhodolith builder. Only the Acervulinid Macroid Accumulation lacks this species.
Remarks: measurements suggest referring this species to *Sporolithon lugeoni* (PFENDER, 1926). However, a designation of species in the current paper seems inappropriate without a general taxonomic revision of Paleogene coralline algae.

Sporolithon sp. B
(Pl. 2, Fig. 4; Pl. 3, Fig. 2)

Thallus morphology see *Sporolithon* sp. A; protuberances (diameter: 1–1.5 mm, height: 1 mm) are

©Verein zur Förderung der Paläontologie am Institut für Paläontologie, Geozentrum Wien

smaller than those of *S.* sp. A.

Anatomy some derivates of the branched core filaments curve outward, but they never curve toward the substrate. Cells are rather small and rarely well developed. Cell length of the core filaments = 14–30 µm (M = 20, SD = 4); cell diameter = 7–13 µm (M = 10, SD = 1.5); ratio cell length/diameter = 1.3–4.3 (M = 2.1, SD = 0.7, N = 20). Cell length of peripheral filaments = 10–14 µm (M = 11, SD = 1.5); cell diameter = 10–13 µm (M = 11, SD = 0.9); ratio cell length/diameter = 0.8–1.3 (M = 1, SD = 0.2, N = 20).

Sporangia: usually not more than 15 conceptacles in one row. The rows are generally less regular and the sporangia are more spherical than those of *S.* sp. A. At the base of the sporangial rows, there is a distinct light row of cells. Up to four filaments are interspersed between the conceptacles, which are not joined to one another. Height of sporangia: 79–108 µm (M = 93, SD = 8); diameter of sporangia = 41–64 µm (M = 52, SD = 6); ratio height/diameter = 1.3–2.4 (M = 1.8, SD = 0.3, N = 20)

Occurrence: besides several fragments, only one specimen could be distinguished in a rhodolith from the upper horizon of the Lower Rhodolith Accumulation.

Remarks: measurements suggest referring this species to *S. nummuliticum* (GÜMBEL) ROTHPLETZ, 1891; for the reasons mentioned above it is not designated.

Order Cryptonemiales SCHMITZ in ENGLER, 1892
Family Peyssonneliaceae DENIZOT, 1968

A recent revision for the Paleogene was undertaken by MOUSSAVIAN (1988).

Genus ***Pseudolithothamnium*** PFENDER, 1936

Cell filaments build a median layer parallel to the substrate. Filaments curve outward and toward the substrate (hypothallus). The perithallus is a thin cell layer above the hypothallus. No calcified sporangia are developed.

Pseudolithothamnium album PFENDER, 1936
(Pl. 2, Fig. 5; Pl. 3, Figs. 5, 6)

1936 *Pseudolithothamnium album* nov. sp. – PFENDER, p. 330, Pl. 19.
1988 *Pseudolithothamnium album* PFENDER – MOUSSAVIAN, S. 100, Abb. 1, Taf. 2, Abb. 2–3.

Thallus morphology smooth crusts without protuberances.

Anatomy superimposed layers with a thickness of more than 0.5 mm each and a golden colour makes this species easy to recognize in thin section. Hypothallus thickness: 100–150 µm; cells elongated, diameter: 19–26 µm, length: 22–45 µm in the centre; about 9–13 µm in diameter, length: 13–22 µm in the peripheral region.

Perithallus: 150–200 µm thick; because of the poor preservation, cells could not be measured. Their dimensions approximately correspond with those of the smaller hypothallus cells.

Occurrence: only in the Lower Rhodolith Accumulation, intergrowing with *Sporolithon* sp. A. It was found to form only one nearly monospecific peyssonneliacean macroid. Fragments are rare.

Class Rhizopoda DUJARDIN, 1841
Order Foraminiferida EICHWALD, 1830
Family Acervulinidae SCHULTZE, 1854
Genus ***Acervulina*** SCHULTZE, 1854

Although HOTTINGER et al. (1993) still differentiate the genera *Gypsina* CARTER, 1877 and *Acervulina* SCHULTZE, 1854, both genera were thought to be congeneric with *Solenomeris* DOUVILLE, 1924 by MOUSSAVIAN & HÖFLING (1993).

Acervulina ogormani (DOUVILLE, 1924)
(Pl. 2, Fig. 8, 9; Pl. 4, Fig. 1, 6, 7)

1918 *Polytrema planum* CARTER – TRAUTH, S. 240, Taf. 3, Abb. 17–18.
1924 *Solenomeris o'gormani* n. gen. n. sp. – DOUVILLE, p. 169–170, Pl. 1–5.
1972 *Gypsina ogormani* (DOUVILLE) – HAGN, S. 116–117, Taf. 8, Fig. 2.
1992 *Solenomeris ogormani* (DOUVILLE) – PLAZIAT & PERRIN, pp. 198–203, Fig. 3–6.

The juvenarium consists of a discoidal stage with large globular chambers. Surrounding chambers are arranged concentrically. Subsequent growth is encrusting and planar, usually parallel to the encrusted substrate. Chambers can be flat or vertically elongated, the roofs appear characteristically convex.

Growth form: laminar and columnar (Ø up to 10 cm)

Occurrence absent in the basal horizon of the Lower Rhodolith Accumulation and in the Upper Rhodolith Accumulation. Forms monospecific macroids in the Acervulinid Macroid Accumulation.

Acervulina linearis (HANZAWA, 1947)
(Pl. 4, Fig. 4)

1947 *Acervulina linearis* HANZAWA – HANZAWA, pp. 60–61, Pl. 16, Fig. 1–2
1992 *Gypsina linearis* HANZAWA – DARGA, S. 61, Taf. 4, Abb. 2.

The juvenarium is comparable to that of *A. ogormani*, but the roofs of the encrusting chambers are not convex and are merged together to form a distinct light line in thin section.

Growth form: laminar crusts; they never become thick (mostly not more than 100–200 µm).

Occurrence: in the whole section but never abundant.

Genus ***Pseudogypsina*** TRAUTH, 1918

Pseudogypsina multiformis TRAUTH, 1918
(Pl. 1, Figs. 1, 2, 5)

1918 *Pseudogypsina multiformis* nov. spec. – TRAUTH, S. 244–245, Taf. 4, Abb. 1–5.

No juvenarium found. Test size: 1–2 mm, chambers flat to high.

©Verein zur Förderung der Paläontologie am Institut für Paläontologie, Geozentrum Wien

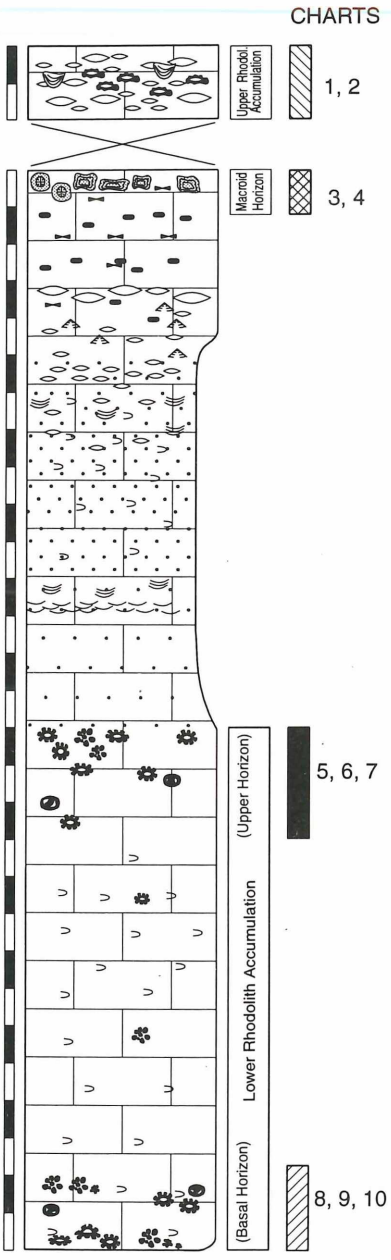

For legend see Fig. 2.

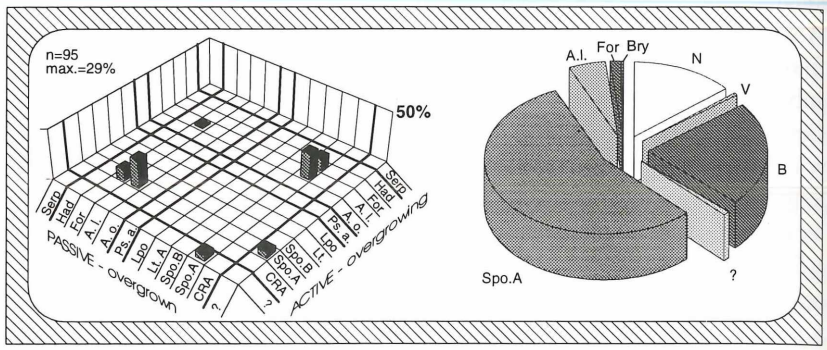

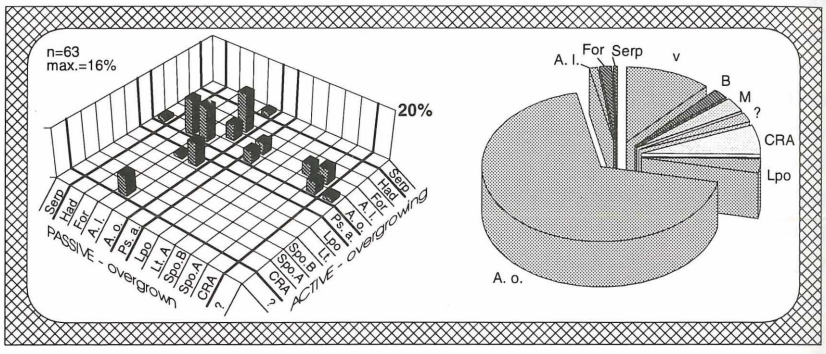

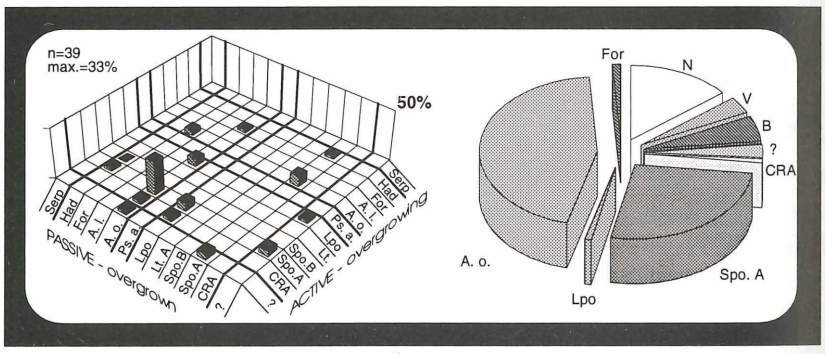

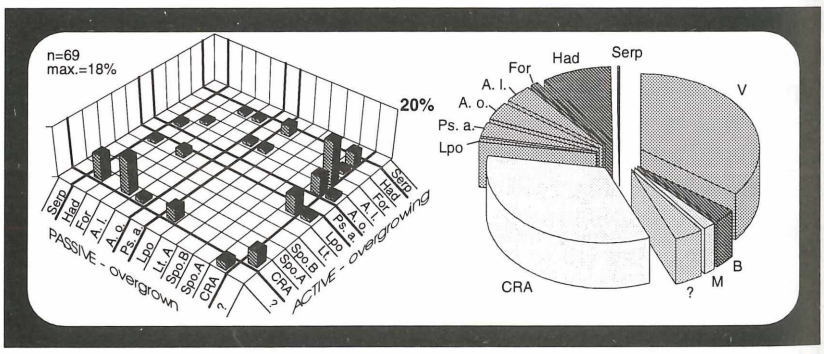

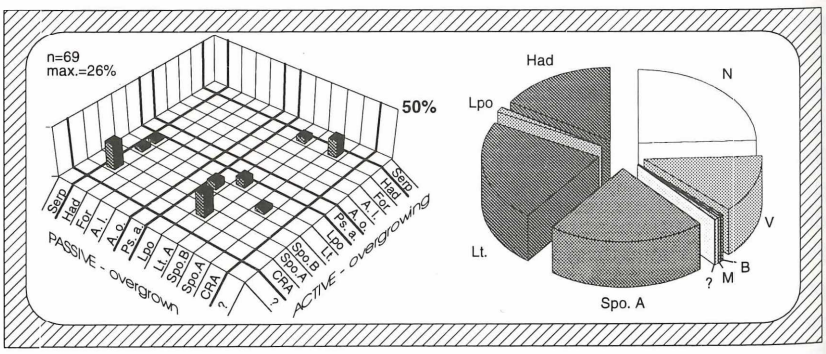

N	nucleus (partially not preserved)
V	voids
B	borings
M	micrite
?	not classified
CRA	unidentified coralline alga
Spo.A	*Sporolithon* sp. A
Spo.B	*Sporolithon* sp. B
Lt	*Lithothamnion* sp.
Lpo	*Lithoporella melobesoides*
Ps. a.	*Pseudolithothamnium album*
A. o.	*Acervulina ogormani*
A. l.	*Acervulina linearis*
For	foraminifera (excl. A.o., A.l., Had)
Had	*Haddonia heissigi*
Serp	serpulid worm tubes
Bry	bryozoans

©Verein zur Förderung der Paläontologie am Institut für Paläontologie, Geozentrum Wien

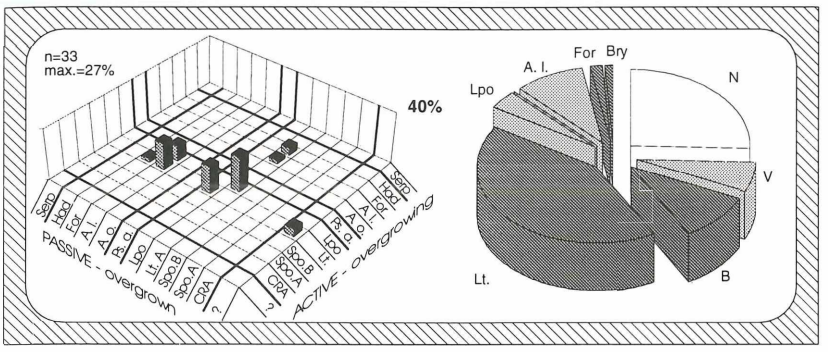

2

Fig. 4: Composition of rhodoliths and macroids (pie charts) and percentage of overgrowths (3–D bars). Each chart (1–10) shows one representative rhodolith; for occurrence in the section see chart numbers.

In the 3–D bars the overgrowing organisms are listed on the right axis and the overgrown ones on the left; the percentage of overgrowths can be read on the intersection. "n" refers to the counted overgrowths, "max." the highest occurring percentage of overgrowths by one taxon in the chart. Percentages are listed in Tab. 1.

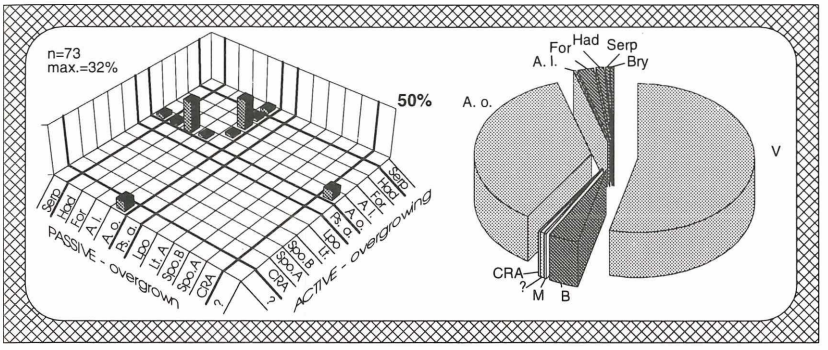

4

For abbreviations see the legend in the lower left corner. The high percentage of "voids" might be caused by borings. Intraspecific overgrowths and crust thickness were not considered. Therefore, species with thin crusts may have a low frequency but a high percentage of overgrowths.

1. Columnar rhodolith, nucleus consists of a *Nummulites* test. "For" are predominantly homotrematid foraminifera. Note the symmetric distribution of the bars (Pl. 2, Fig. 7) (sample UF1).

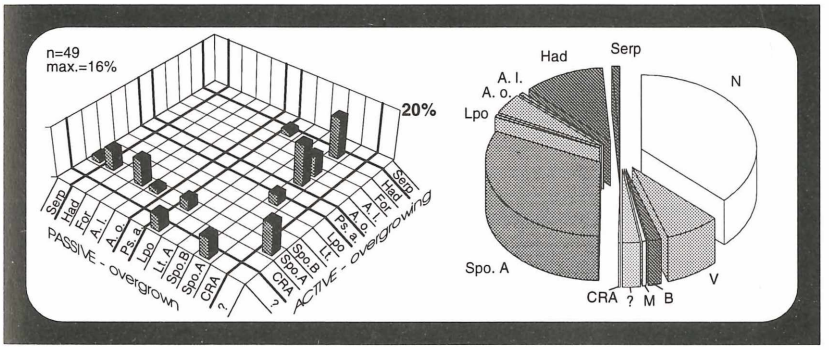

6

2. Rhodolith with a *Nummulites* - nucleus (sample no. UF2B).

3. Acervulinid macroid (Ø > 3 cm); inner part laminar-concentric, outermost part with smooth protuberances. *L. melobesioides* shows, atypically, 11 consecutive layers. "For" are predominantly homotrematid foraminifera. "CRA" serves as a nucleus (Pl. 3, Fig. 3) (sample no. H9–3B).

4. Columnar acervulinid macroid (Ø > 10 cm); note the extremely symmetrical distribution of the 3–D charts. "For" are predominantly homotrematid foraminifera and (less frequently) other sessile rotaliid foraminifera (Fig. 4; Pl. 2, Fig. 9) (sample no. H9–5B).

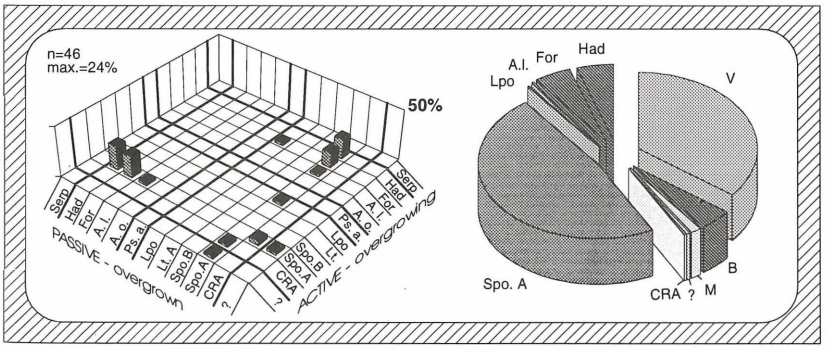

8

5. Columnar rhodolith (resp. macroid), Ø > 4 cm. Outermost layer consists of columnar "Spo.A", partially the columns join laterally. "N" is a sediment-filled void (sample no. A18A).

6. Columnar rhodolith. *A. ogormani* forms the final crust. The nucleus is partially sediment-filled and shows relict structures of a coral (sample no. A18C).

7. Very heterogeneous laminar rhodolith with destroyed internal structure and ellipsoidal shape (Ø 6 cm) (sample no. A20).

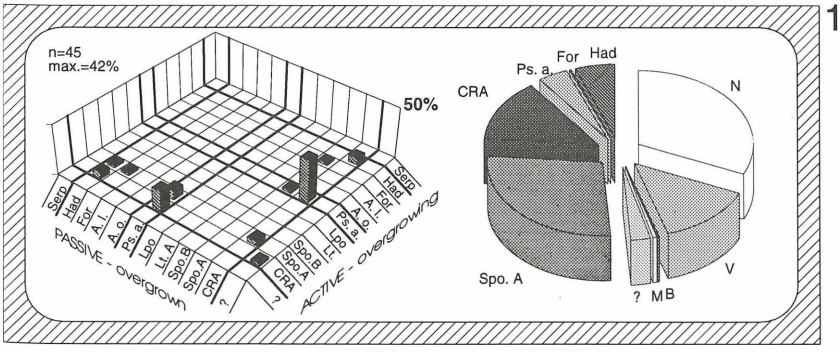

10

8. Branched rhodolith, Ø > 5 cm. The space between the branches was counted as "voids" within the contour of the rhodolith. "For" are dominated by the sessil foraminifer *Fabiania cassis* (OPPENHEIM, 1896). (Pl. 2, Fig. 3) (sample no. F3).

9. Columnar rhodolith (Ø 4 cm) with coral nucleus (Pl. 2, Fig. 6) (sample no. F3).

10. Columnar rhodolith (Ø 4 cm), irregular shape. The nucleus is preserved as a sediment-filled void (sample no. F3B).

©Verein zur Förderung der Paläontologie am Institut für Paläontologie, Geozentrum Wien

Passive - OVERGROWN / Active - OVERGROWING

	Serp	Had	For	A.I.	A.o.	Ps.a.	Lpo	Lt.	Spo.B	Spo.A	CRA	?
?										5,5		
CRA												
Spo.A			11,5	28,8								5,5
Spo.B												
Lt.												
Lpo												
Ps.a.												
A.o.												
A.I.			1,5							26,5		
For										12,5		
Had												
Serp												

Chart 1, sample no. UF1. Percentages of overgrowings (left side) and frequencies of rhodolith constituents (below)

N	14,0		
V	0,6	Lpo	
B	22,5	Ps.a.	
M		A.o.	
?	0,8	A.I.	4,8
CRA		For	1,4
Spo.A	55,7	Had	
Spo.B		Serp	
Lt.		Bry	0,2

Passive - OVERGROWN / Active - OVERGROWING

	Serp	Had	For	A.I.	A.o.	Ps.a.	Lpo	Lt.	Spo.B	Spo.A	CRA	?
?								6,0				
CRA												
Spo.A												
Spo.B												
Lt.			3,0	21,2			21,2					6,0
Lpo				12,1				27,3				
Ps.a.												
A.o.												
A.I.								3,0				
For								6,0				
Had												
Serp												

Chart 2, sample no. UF2. Percentages of overgrowings (left side) and frequencies of rhodolith constituents (below)

N	25,8		
V	6,3	Lpo	3,9
B	10,2	Ps.a.	
M		A.o.	
?		A.I.	9,4
CRA		For	1,6
Spo.A		Had	
Spo.B		Serp	
Lt.	42,0	Bry	0,8

Passive - OVERGROWN / Active - OVERGROWING

	Serp	Had	For	A.I.	A.o.	Ps.a.	Lpo	Lt.	Spo.B	Spo.A	CRA	?
?												
CRA				7,9								
Spo.A												
Spo.B												
Lt.												
Lpo				1,6	9,5							
Ps.a.												
A.o.	1,6		14,3	14,3			4,8				4,8	1,6
A.I.					6,3		4,8			4,8	6,3	
For					15,9							
Had												
Serp					1,6							

Chart 3, sample no. H9-3. Percentages of overgrowings (left side) and frequencies of rhodolith constituents

N			
V	11,8	Lpo	3,1
B	2,3	Ps.a.	
M	3,1	A.o.	68,3
?	1,9	A.I.	1,2
CRA	6,2	For	1,7
Spo.A		Had	
Spo.B		Serp	0,4
Lt.		Bry	

Passive - OVERGROWN / Active - OVERGROWING

	Serp	Had	For	A.I.	A.o.	Ps.a.	Lpo	Lt.	Spo.B	Spo.A	CRA	?
?					9,6							
CRA												
Spo.A												
Spo.B												
Lt.												
Lpo												
Ps.a.												
A.o.	4,1	1,4	31,5	2,7								9,6
A.I.					2,7							
For					30,1							
Had					2,7							
Serp					4,1							

Chart 4, sample no. H9-5. Percentages of overgrowings (left side) and frequencies of rhodolith constituents

N			
V	54,0	Lpo	
B	4,3	Ps.a.	
M	0,3	A.o.	36,2
?	0,5	A.I.	0,3
CRA	0,1	For	2,3
Spo.A		Had	1,0
Spo.B		Serp	0,7
Lt.		Bry	0,3

Passive - OVERGROWN / Active - OVERGROWING

	Serp	Had	For	A.I.	A.o.	Ps.a.	Lpo	Lt.	Spo.B	Spo.A	CRA	?
?					2,6					5,1		
CRA					2,6		2,6					
Spo.A		2,6			33,0		7,6					5,1
Spo.B												
Lt.												
Lpo					7,6							2,6
Ps.a.												
A.o.			5,1							10,3		
A.I.												
For					2,6							
Had										2,6		
Serp												

Chart 5, sample no. A18A Percentages of overgrowings (left side) and frequencies of rhodolith constituents

N	14,4		
V	3,5	Lpo	0,9
B	5,5	Ps.a.	
M		A.o.	44,7
?	2,8	A.I.	
CRA	0,8	For	0,8
Spo.A	26,5	Had	
Spo.B		Serp	
Lt.		Bry	

Passive - OVERGROWN / Active - OVERGROWING

	Serp	Had	For	A.I.	A.o.	Ps.a.	Lpo	Lt.	Spo.B	Spo.A	CRA	?
?							6,1			8,1		
CRA												
Spo.A	2,0	8,1		10,2	2,0		4,1					12,2
Spo.B												
Lt.												
Lpo										4,1		
Ps.a.												
A.o.										16,3		
A.I.										8,1		
For												
Had										16,3		
Serp												

Chart 6, sample no. A18C. Percentages of overgrowings (left side) and frequencies of rhodolith constituents

N	37,3		
V	7,7	Lpo	0,5
B	2,0	Ps.a.	
M	0,5	A.o.	4,5
?	2,5	A.I.	0,5
CRA	0,3	For	
Spo.A	31,9	Had	11,3
Spo.B		Serp	1,0
Lt.		Bry	

Passive - OVERGROWN / Active - OVERGROWING

	Serp	Had	For	A.I.	A.o.	Ps.a.	Lpo	Lt.	Spo.B	Spo.A	CRA	?
?											2,9	
CRA												5,8
Spo.A		10,0		14,5	1,4		5,8					
Spo.B												
Lt.												
Lpo		1,4		2,9							7,2	1,4
Ps.a.												
A.o.		1,4									7,2	1,4
A.I.			1,4			1,4	1,4				17,4	
For											1,4	
Had				1,4	1,4		4,3				5,8	
Serp												

Chart 7, sample no. A20. Percentages of overgrowings (left side) and frequencies of rhodolith constituents (below)

N			
V	35,5	Lpo	1,0
B	3,0	Ps.a.	3,0
M	1,6	A.o.	4,0
?	3,8	A.I.	3,8
CRA	33,6	For	1,0
Spo.A		Had	9,5
Spo.B		Serp	2,0
Lt.		Bry	

Passive - OVERGROWN / Active - OVERGROWING

	Serp	Had	For	A.I.	A.o.	Ps.a.	Lpo	Lt.	Spo.B	Spo.A	CRA	?
?										2,2		
CRA										2,2		
Spo.A		24,0	21,7	2,2							4,3	2,2
Spo.B												
Lt.												
Lpo										2,2		
Ps.a.												
A.o.												
A.I.										2,2		
For							2,2			15,2		
Had										19,6		
Serp												

Chart 8, sample no. F2. Percentages of overgrowings (left side) and frequencies of rhodolith constituents (below)

N			
V	35,7	Lpo	0,1
B	4,4	Ps.a.	
M	1,5	A.o.	
?	0,5	A.I.	0,1
CRA	0,3	For	4,9
Spo.A	47,5	Had	4,9
Spo.B		Serp	
Lt.		Bry	

Passive - OVERGROWN / Active - OVERGROWING

	Serp	Had	For	A.I.	A.o.	Ps.a.	Lpo	Lt.	Spo.B	Spo.A	CRA	?
?												
CRA								23,2				
Spo.A		26,0										
Spo.B												
Lt.		4,3					7,2			4,3		
Lpo		2,9						8,7				
Ps.a.												
A.o.												
A.I.												
For												
Had								5,8		17,4		
Serp												

Chart 9, sample no. F3. Percentages of overgrowings (left side) and frequencies of rhodolith constituents (below)

N	24,6		
V	12,7	Lpo	1,0
B	0,7	Ps.a.	
M	0,1	A.o.	
?	0,6	A.I.	
CRA		For	
Spo.A	21,8	Had	16,1
Spo.B		Serp	
Lt.	22,4	Bry	

Passive - OVERGROWN / Active - OVERGROWING

	Serp	Had	For	A.I.	A.o.	Ps.a.	Lpo	Lt.	Spo.B	Spo.A	CRA	?
?												
CRA		6,7				20,0						2,2
Spo.A		2,2	2,2			8,9					4,4	
Spo.B												
Lt.												
Lpo												
Ps.a.											42,2	
A.o.												
A.I.												
For										2,2		
Had											6,7	
Serp												

Chart 10, sample no. F3B. Percentages of over- growings (left side) and frequencies of rhodolith constituents

N	31,9		
V	13,6	Lpo	
B	0,1	Ps.a.	4,1
M	0,7	A.o.	
?	2,6	A.I.	
CRA	13,7	For	0,4
Spo.A	27,5	Had	5,4
Spo.B		Serp	
Lt.		Bry	

Table 1: Percentages of overgrowths (3–D charts) and frequencies of rhodoliths/macroid constituents (pie charts). For abbreviations see Fig. 4.

©Verein zur Förderung der Paläontologie am Institut für Paläontologie, Geozentrum Wien

Growth form: tests U-shaped in thin section (growth form: half-tube; Pl. 1, Fig. 2). Never found attached to a substrate.
Occurrence: characterizing three sedimentary facies (Rhodolith–*Pseudogypsina* Facies, *Pseudogypsina* Facies, Siliciclastic *Pseudogypsina* Facies).

8. Encrusting communities

Most rhodoliths are coated grains predominantly consisting of nongeniculate encrusting coralline red algae (Corallinaceae, Rhodophyta) (BOSELLINI & GINSBURG, 1971; BOSENCE, 1983a). Consequently, coated grains composed of peyssonneliacean algae are to be termed "macroids".
The term macroid was defined by PERYT (1983) to describe the size of coated grains (Ø > 10 mm). Usually, however, it is applied to coated grains composed of non coralline algal organisms (e.g., HOTTINGER, 1983). In the current paper, coated grains largely consisting of acervulinid foraminifera are called acervulinid macroids. The terms of growth forms are used according to BOSENCE (1983a). The terms "columnar" and "laminar", used for rhodoliths, also are applied to acervulinid macroids (no branched macroids were detected).

8.1. Lower Rhodolith Accumulation

The Lower Rhodolith Accumulation can be divided into two horizons with corresponding growth form, shape, size and, partially, taxonomic composition. The basal horizon (Rhodolith – *Pseudogypsina* Facies) is equally developed and outcropped in both partial section A and F (compare Fig. 1). In the overlying *Pseudogypsina* Facies, rhodoliths are less frequent; however, several small accumulations can be found in all partial sections. The upper horizon (Rhodolith Facies) only occurs in section A. Section C instead shows a transition from the under– to the overlying facies, with rare rhodoliths but a higher amount of rhodolith fragments.
The **dominant encrusting organism** is *Sporolithon* sp. A, forming nearly monospecific rhodoliths (up to 48 % of the rhodoliths: Fig. 4). *Sporolithon* sp. B was found in only one rhodolith of the upper horizon and in several fragments. Other coralline algae include *Lithothamnion* sp. (only found in one rhodolith with 22 %) and *Lithoporella melobesioides* (up to 1 %). *Pseudolithothamnium album* was found to form only one nearly monospecific macroid (Pl. 2, Fig. 5) and is generally rare in rhodoliths (3–4 %). Fragments of this species are rare. Acervulinid foraminifera occur in rhodoliths in varying frequencies. *Acervulina ogormani* is common (up to 45 %), but absent in the basal horizon. *Acervulina linearis* occurs in rhodoliths of the whole accumulation (max. 4 %).
Other sessile organisms: The agglutinated foraminifer *Haddonia heissigi* (Pl. 4, Figs. 4, 5) is the most common. Serpulid worm tubes are rare.
Nuclei: Coral fragments are common nuclei (Pl. 2, Fig. 6); often only relict structures are visible. In many cases nuclei are not preserved and their voids are filled with sediment (Pl. 2, Fig. 1). Most of them might have been leached corals although soft plants are also possible.
Growth forms: (1) Columnar rhodoliths forming short, stubby protuberances (height: 10–20 mm, diameter: 3–10 mm) are the most common. They are dominated by *Sporolithon* sp. A. Encrustation of nuclei begins with a 0.5–1 mm thick laminar stage followed by columnar growth. The rhodoliths (Ø up to 6 cm) are predominantly spheroidal; sometimes the shape is influenced by the nucleus. *Acervulina ogormani* tends to smooth the relief of coralline algal protuberances. (2) Ellipsoidal laminar rhodoliths (Ø up to 6 cm, e.g. Fig. 4, chart 7) are rare. Their internal structure is mostly destroyed by borings. Generally no nucleus is visible. (3) Branched rhodoliths (Ø up to 5 cm, Pl. 2, Fig. 3) are the least common; generally no nucleus is visible. Dichotomous branching is not dense (branching I–II according to BOSENCE, 1983a).
Growth succession: Coralline algae (mostly *Sporolithon* sp. A) generally form thick continuous crusts in the basal horizon. Only in the upper horizon is *Acervulina ogormani* intercalated with coralline algae and may even dominate rhodoliths (macroids). A few of the columnar rhodoliths between the horizons (*Pseudogypsina* Facies) are characterized by final acervulinid layers. Both *Lithoporella melobesioides* and *Acervulina linearis* form thin intercalations (only 1–2 layers).

8.2. Acervulinid Macroid Accumulation

The Acervulinid Macroid Accumulation lacks rhodoliths. Macroids of the U- and H-section are different. The partial section H is dominated by large columnar rhodoliths, partial section U by small laminar rhodoliths with well preserved coral nuclei.
Encrusting organisms: The dominant species is *Acervulina ogormani* (up to 68 %), forming nearly monospecific macroids. The contribution of *Acervulina*

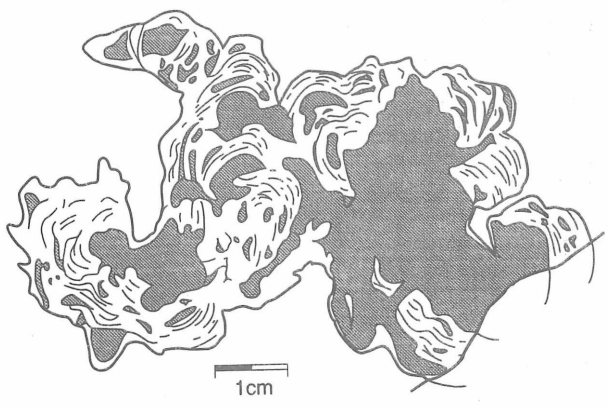

Figure 5: Acervulinid macroid predominantly consisting of *Acervulina ogormani* (Fig. 4, chart 4; Pl. 2, Fig. 9). Greyish colour: sediment-filled voids. Note the distinct growth directions.

©Verein zur Förderung der Paläontologie am Institut für Paläontologie, Geozentrum Wien

linearis is never more than 1 %. *Lithoporella melobesioides* (max. 3%) is the only coralline alga in this accumulation. Bryozoans are restricted to the macroids of this accumulation, but they are rare (0.3 %).

Other sessile organisms: Homotrematid foraminifera (up to 2.2 %) and serpulid worm tubes (0.4–0.7 %) have their greatest abundance here. The agglutinated foraminifer *Haddonia heissigi* is absent within the acervulinid macroids.

Nuclei: Coral fragments are the most common nuclei. In most cases they are dissolved and the voids are filled with sediment. Only one coralline algal fragment was found to serve as a nucleus (Fig. 4, chart 3).

Growth forms: (1) The larger the macroids are, the more they tend to be columnar. They can be very large (Ø up to 10 cm, Fig. 5; Pl. 2, Fig. 9) with irregular shape and distinct growth directions. (2) Laminar concentric macroids (Ø not more than 3 cm, Pl. 2, Fig. 8) with well preserved coral-nuclei are less common. They are mostly spheroidal and predominantly occur in partial section U.

Growth succession: Acervulinid macroids are largely monospecific. Their thick crusts are mostly intergrown with homotrematid foraminifera and serpulid worm tubes (Pl. 4, Figs. 6, 7) and show characteristic borings (Pl. 4, Fig. 3). *Acervulina linearis* and *Lithoporella melobesioides* usually show only 1–2 layers. In one case the latter had 11 consecutive layers (Pl. 3, Fig. 3).

8.3. Upper Rhodolith Accumulation

Encrusting organisms: The dominant encrusting organism is *Sporolithon* sp. A (up to 56 %: Pl. 2, Fig. 7). *Lithothamnion* sp. dominates one rhodolith (42 %; Fig. 4, chart 2), but it is the only recognized occurrence. *Lithoporella melobesioides* contributes up to 4 %. *Acervulina ogormani* is absent, but *Acervulina linearis* (up to 9 %) has its maximum in the section here.

Nuclei: The only nuclei are large tests (probably microspheric generation) of *Nummulites* div. spec. Perhaps large tests are preferred, as they are turned less frequently than smaller ones.

Growth forms: Laminar to columnar. The larger the rhodoliths, the more distinct the columns. The shape is ellipsoidal and influenced by the nucleus shape.

9. Discussion

9.1. Facies division

The Krappfeld Paleogene was recently studied by WILKENS (1989, 1991), who established new lithostratigraphic units (fig. 2) and facies divisions (Fig. 6). The latter could be roughly confirmed in the current study. Parts of the facies sequence and some facies trends in WILKENS (1991), however, could not be reconstructed. This might be due to either the permanently changing

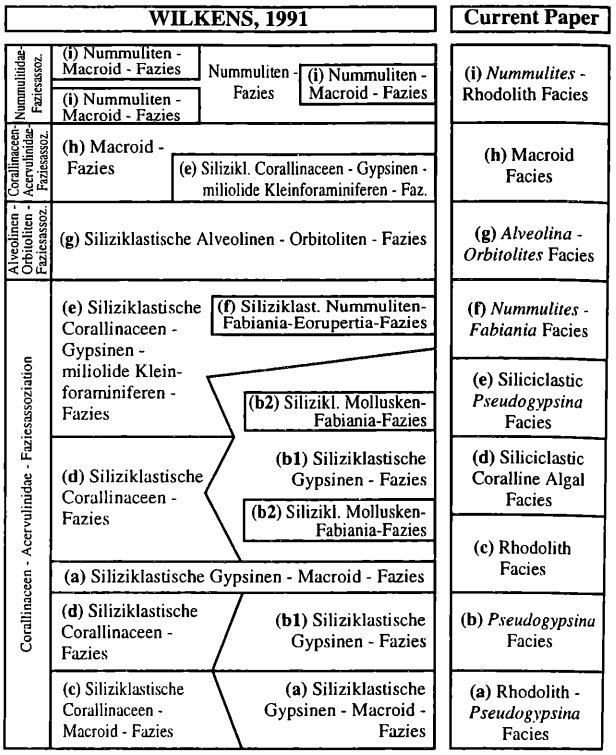

Figure 6: Facies division of WILKENS (1991), compared to the current paper. Facies are arranged according to stratigraphic position (not to scale). Characters (a–i) designate the corresponding facies.

outcrop situation in the Fuchsofen quarry or the lacking detailed documentation of the samples' origin in the cited paper.

Samples analysed in the current study (Fig. 1 and 3) and nomenclatural differences in some cases suggest new facies names (characters a-i are referred to the facies in Fig. 6).

One difference is that WILKENS (1991) differentiates between rhodoliths and (acervulinid) macroids in facies descriptions. This differentiation, however, is not considered in his facies denomination (facies (a), (c) and (i) are dominated by rhodoliths, facies (h) by acervulinid macroids).

The terrigenous content of facies (a) and (b) is rather low compared with facies (e). Therefore it should not be considered in the facies names.

The term "Gypsinen" (facies (a), (b), and (e)) is avoided in the current paper. On one hand, the genus *Gypsina* is rejected (MOUSSAVIAN & HÖFLING, 1994) and WILKENS also does not use it; on the other hand this term is not common in the literature.

Facies (b.2) could not be differentiated, as *Fabiania* has no distinct maximum in abundance and mollusc accumulations are distributed regularly.

Facies (f): the foraminifer *Eorupertia* could not be found. The "Nummuliten-Fazies" (WILKENS) cannot be distinguished.

©Verein zur Förderung der Paläontologie am Institut für Paläontologie, Geozentrum Wien

9.2. Rhodoliths and related facies

The most important limiting factor for the distribution of coralline algae seems to be **light intensity**, correlated with depth and geographical latitude. Living specimens were found below 200 m (ADEY & MACINTYRE, 1973; LITTLER et al., 1991), but 80 m is the typical limit in the tropics, and 20–40 m in colder climates (ADEY, 1986) and higher latitudes, respectively. The dominating rhodolith builder in the study area is *Sporolithon*. In the Recent, this genus prefers low-light conditions and thus is most abundant between 30 and 50 m in the tropics (ADEY & MACINTYRE, 1973; WRAY, 1977; ADEY, 1979; MINNERY et al., 1985; ADEY, 1986; MANKER & CARTER, 1987; FRAVEGA et al., 1989). Deeper water genera also occur in cryptic shallow water environments (BOSENCE, 1983b). Therefore, TABERNER & BOSENCE (1985) interpret the presence of *Sporolithon* in an Eocene (shallow water) patch reef to be correlated with a high water turbidity, since ADEY (1979) stated that the distribution of Recent and Paleogene coralline algal genera is similar. However, the question is whether actuopalaeontological statements for coralline algae are valid on generic level. On one hand, coralline algal species are quite different in the Recent and the Paleogene, on the other, FRAVEGA et al. (1989) showed on two recent species of *Sporolithon* that a single species may occur in the uppermost subtidal as well as below 50 m. Consequently, a reconstruction of the depth using coralline algae without incorporating further depth indicators seems inappropriate.

In the study section, larger miliolid foraminifera and nummulites generally point to a shallow water environment (LUTERBACHER, 1982). The *Nummulites – Fabiania* Facies (lacking rhodoliths) can be identified as a nummulite bank facies (sensu AIGNER, 1983) and therefore should be restricted to very shallow water. Equally, micrite envelopes in all facies (except the *Nummulites* - Rhodolith Facies) require warm and shallow water environments (BATHURST, 1971; FÜCHTBAUER & RICHTER, 1988; TUCKER & WRIGHT, 1990) in view of the necessary availability of light and $CaCO_3$.

Temperature is the second important factor for coralline algal distribution (BOSENCE, 1983b). ADEY & MACINTYRE (1973), WRAY (1977), BOSENCE (1983b), and MANKER & CARTER (1987) classify *Sporolithon* as a typical warm water genus, and FRAVEGA et al. (1989) delimit it to 20°N and 30°S in the Recent. For the study section, the general paleogeography of the Paleogene (MCGOWRAN, 1989), the micrite envelopes of several components, and the larger foraminifera support the hypothesis of a tropical to subtropical environment.

Water energy is another important ecological factor for coralline algal distribution. On one hand, it may influence the distribution of herbivorous animals (STENECK, 1985). On the other, it controls rhodolith formation (growth form, taxonomic succession) (BOSELLINI & GINSBURG, 1971; BOSENCE & PEDLEY, 1982; BOSENCE, 1984; BRAGA & MARTIN, 1988; BOSENCE, 1991).

Growth form and shape of rhodoliths are apparently controlled predominantly by the frequency of turning (BRAGA & MARTIN, 1988; BOSENCE, 1991). This is confirmed by the observation of BOSELLINI & GINSBURG (1971) that an increasing frequency of rhodolith turning causes a flattening of the branches, which then join together laterally. In the Lower Rhodolith Accumulation of the study section, most rhodoliths show laterally growing (flat) columns. Only a few columnar rhodoliths with laterally joining protuberances where found. Branching is dichotomous, never intercalary. Both column shape and branching type indicate moderate water energy (BOSENCE, 1983b). The energy index after PLUMLEY et al. (1962) confirms this interpretation, pointing to "moderately agitated": particles (predominantly coarse sand) are mostly well rounded and grainstone dominates over packstone (except for the *Nummulites* - Rhodolith Facies).

Rhodoliths of the Upper Rhodolith Accumulation show small columns without lateral growth. As discussed above, such a growth form points to low water energy. This interpretation is supported by the high percentage of (unwinnowed) micritic matrix. However, the occurrence of unrounded bioclasts together with a micritic matrix suggests a textural inversion caused by excessive water energy (FOLK, 1962). On the other hand, the rhodoliths show neither abrasion nor fragmentation caused by transportation. Additionally, bioclasts could also be produced by biogenic activities. The poor outcrop situtation does not allow this inconsistency to be solved

Taxonomic successions may be the result of a change in rhodolith size (the larger the size, the higher their stability) rather than environmental change (ADEY & MACINTYRE, 1973). This is supported by BOSENCE (1983b), who observed that smaller rhodoliths generally have a different encrusting flora than larger ones. Rhodoliths in parts of the Lower Rhodolith Accumulation are characterized by intercalations of *Acervulina ogormani*, with increasing abundance upsection. However, abundance is independent of rhodolith size. Therefore another factor most likely influences their distribution. Comparable growth successions are well known in recent rhodoliths (LOGAN et al., 1969; TOOMEY, 1975; REID & MACINTYRE, 1988) and interpreted as a response to Holocene sea level rise. Moreover, PERRIN (1992) points out that acervulinid foraminifera are best developed in environments where ecological conditions lead to reduced competition. In the study section this could be caused by a light reduction accompanying a deepening of the environment.

©Verein zur Förderung der Paläontologie am Institut für Paläontologie, Geozentrum Wien

9.3. Acervulinid macroids and related facies

Several studies document recent laminar acervulinid macroids in deeper water (HOTTINGER, 1983; REID & MACINTYRE, 1988; PILLER & PERVESLER, 1989). However, documentations of columnar macroids are rare (PERRIN, 1992; PLAZIAT & PERRIN, 1992). Apparently nothing is known about photosynthetic symbionts in acervulinid foraminifera and thus about their possible dependence on light. Nevertheless, depth distribution of Paleogene acervulinid foraminifera can be reconstructed based on growth form (HÖFLING & MOUSSAVIAN, 1990; MOUSSAVIAN & HÖFLING, 1993): macroids with distinct protuberances grow predominantly in the upper subtidal, laminar macroids in the lower subtidal. For the study section, irregular growth forms and distinct growth directions of the columnar macroids (Fig. 5; Pl. 2, Fig. 9) in the Acervulinid Macroid Accumulation point to a low frequency of turning. According to SCOFFIN et al. (1985), massive rhodoliths and macroids in an environment influenced by strong tidal currents (up to 90 cm/s) were not observed to turn. Nevertheless, the authors assume periodical turning because of the regular shape. The larger miliolid foraminifer *Orbitolites* suggests the occurrence of seagrass (HOTTINGER, 1973; BRASIER, 1975; EVA, 1980), which would stabilize the macroids. However, infrequent turning may also refer to a low water energy environment.

10. Conclusions

Sediments of the study section were deposited in a highly structured tropical to subtropical environment with rapid lateral facies changes.

Sedimentological parameters and the abundance of micrite envelopes indicate a shallow water environment for the Lower Rhodolith Accumulation. Intertidal and lower subtidal can be excluded, since free columnar growth forms and dichotomous branching of rhodoliths – together with the energy index after PLUMLEY et al. (1962) – point to moderately agitated water rather than a very high or very low energy environment. Coralline algae provide no absolute depth data, but the increasing upward abundancy of intercalating acervulinid foraminifera in the section suggests a deepening from the Rhodolith *Pseudogypsina* Facies to the Rhodolith Facies.

The Siliciclastic Coralline Algal Facies and the Siliciclastic *Pseudogypsina* Facies are strongly terrigenously influenced. This high input is probably responsible for the absence of rhodoliths and acervulinid macroids.

The *Nummulites–Fabiania* Facies can be interpreted as a nummulite bank facies (AIGNER 1983). This indicates a shoal facies with in situ winnowing of nummulite buildups. No rhodoliths or acervulinid macroids occur.

The *Alveolina–Orbitolites* Facies is dominated by packstones. This indicates low water energy and/or stabilization and sediment baffling by seagrass. Columnar macroids of the Acervulinid Macroid Accumulation were turned infrequently. They probably grew in a protected shallow water environment stabilized by seagrass.

The sediment of the *Nummulites*–Rhodolith Facies is a packstone; sparry cement is rare. Thus a nummulite bank facies with in situ winnowing is improbable. The nummulite tests are often encrusted by coralline algae forming the Upper Rhodolith Accumulation. The small columns of the rhodoliths and the muddy matrix indicate a very low energy environment.

Acknowledgements

This paper is dedicated to Astrid. I am particularly grateful to W. E. Piller (Institute for Palaeontology, Univ. Vienna) for his encouragement to write this paper, his supports in field work, the comprehensive stimulating discussions and critical readings of the manuscript. I am also indebted to F.F. Steininger (Institute for Palaeontology, Univ. Vienna) for the discussions of stratigraphic problems. Sincere thanks to A. Freiwald (Univ. Bremen, Fachber. Geowissenschaften) and E. Moussavian (Institute for Palaeont. and Hist. Geol., Univ. München) for the reviews and constructive discussions and to M. Stachowitsch (Institute for Zoology, Univ. Vienna) for the correction of the English. Thin sections were prepared by F. Sattler, V. Perlinger and W. Simeth, photographs printed by R. Gold. This study was supported by the Wietersdorfer & Peggauer Zementwerke Knoch, Kern & Co. (Wietersdorf), the IGCP Project 308, and the "Amt der Kärntner Landesregierung, Kulturabteilung"

11. References

ADEY, W H., 1986. Coralline algae as indicators of sea-level. – [in:] PLASCHE, O. van de (ed.): Sea-level research, a manual for the collection and evaluation of data. — :229–280, Norwich (Geo Books).

ADEY, W. H. & MACINTYRE, I. G., 1973. Crustose coralline algae: A re-evaluation in the geological sciences. — Geol. Soc. Amer. Bulletin, **84**:883–904, Boulder.

ADEY, W. H., 1979. Crustose coralline algae as microenvironmental indicators for the Tertiary. – [in:] GRAY, J. & BOUCOT, A. J. (eds.): Historical biogeography. — :459–464, Oregon (Oregon State Univ. Press).

AIGNER, T., 1983. Facies and origin of nummulitic buildups: an example from the Giza Pyramids Plateau (Middle Eocene, Egypt). — N. Jb. Geol. Paläont. Abh., **166**(3):347–368, Stuttgart.

BACCELLE, L. & BOSELLINI, A., 1965. Diagrammi per la stima visiva della composizione percentuale nelle rocce sedimentarie. — Ann. Univ. Ferrara, N.S., Sez. IX, Sci. Geol. Paleont., **1**(3):59–62, Ferrara.

BATHURST, R. G. C., 1971. Carbonate sediments and their diagenesis. — XIX + 620 pp., (Elsevier) Amsterdam – London – New York.

BOSELLINI, A. & GINSBURG, R. N., 1971. Form and internal structure of recent algal nodules (rhodolites)

©Verein zur Förderung der Paläontologie am Institut für Paläontologie, Geozentrum Wien

from Bermuda. — Journal of Geology, **79**:669–682, Chicago.

BOSENCE, D. W. J., 1983a. Description and Classification of Rhodoliths. – [in:] PERYT, T. M. (ed.): Coated Grains. — :217–224, Berlin – Heidelberg (Springer).

BOSENCE, D. W. J., 1983b. The Occurrence and Ecology of Recent Rhodoliths. – [in:] PERYT, T. M. (ed.). Coated Grains. — :225–242, Berlin – Heidelberg (Springer).

BOSENCE, D. W. J., 1983c. Coralline algae from the Miocene of Malta. — Palaeont., **26**(1):147–173, London.

BOSENCE, D. W. J., 1984. Construction and preservation of two modern coralline algal reefs, St. Croix, Caribbean. — Palaeontology, **26**(1):147–574, London.

BOSENCE, D. W. J., 1991. Coralline Algae: Mineralization, Taxonomy and Palaeoecology. – [in:] RIDING, R. (ed.). Calcareous Algae and Stromatolites. — :98–113, Berlin – Heidelberg (Springer).

BOSENCE, D. W. J. & PEDLEY, H. M., 1982. Sedimentology and palaeoecology of a Miocene coralline algal biostrome from the Maltese Islands. — Palaeogeogr. Palaeoclimatol. Palaeoecol. **38**:9–43, Amsterdam.

BRAGA, J. C. & MARTIN, J. M., 1988. Neogene coralline-algal growth-forms and their palaeoenvironments in the Almanzora river valley (Almeria, S.E. Spain). — Palaeogeogr. Palaeoclimatol. Palaeoecol., **67**:285–303, Amsterdam.

BRASIER, M. D., 1975. Ecology of recent sediment-dwelling and phytal foraminifera from the lagoons of Barbuda, West Indies. — J. Foram. Res., **5**(1):42–62, Lawrence.

DARGA, R., 1992. Geologie, Paläontologie und Palökologie der südostbayerischen unter-priabonen (Ober-Eozän) Riffkalkvorkommen des Eisenrichtersteins bei Hallthurm (Nördliche Kalkalpen) und des Kirchbergs bei Neubeuern (Helvetikum). — Münchner Geowiss. Abh., (A)**23**:1–166. München.

DOUVILLE, H., 1924. Un nouveau genre d'Algues calcaires. — C. R. Somm. Soc. Géol. Fr., **4**:169–170, Paris.

DUNHAM, R. J., 1962. Classification of carbonate rocks according to depositional texture. — Mem. Amer. Ass. Petrol. Geol., **1**:108–121, Tulsa.

EMBRY, A. F. & KLOVAN, J. E., 1972. Absolute Depth Limits of Late Devonian Paleoecological Zones. — Geol. Rundschau, **61**: 672–686, Stuttgart.

EVA, A. N., 1980. Pre-Miocene seagrass communities in the Caribbean. — Palaeontology, **23**:231–236, London.

FAUPL, P., POBER, E. & WAGREICH, M., 1987. Facies development of the Gosau Group of the eastern parts of the Northern Calcareous Alps during the Cretaceous and Paleogene. – [in:] Flügel, H. W. & Faupl, P. (eds.): Geodynamic of the Eastern Alps. — :142–155, Wien (Deutike).

FOLK, R. L., 1962. Spectral subdivision of limestone types. — Amer. Ass. Petrol. Geol., **1**: 62–84, Tulsa.

FRAVEGA, P., PIAZZA, M. & VANNUCCI, G., 1989. *Archaeolithothamnium* ROTHPLETZ, Indicatore Ecologico – Stratigrafico? — Atti 3. Simposio di Ecologia e Paleoecologia delle Comunitá Bentoniche 1985, Estratto :729–743, Catania.

FÜCHTBAUER, H. & RICHTER, D. K., 1988. Karbonatgesteine. – [in:] FÜCHTBAUER, H. (ed.). Sedimente und Sedimentgesteine. — :233–434, Stuttgart (Schweizerbart).

GOSEN, W. von, 1989. Tektonisch-metamorphe Entwicklung der Gesteinsserien des Mittel- und Oberostalpins auf ÖK-Blatt 126 St. Veit/Glan. — Arbeitstagung Geol. B.-A., **1989**:80–84, Wien.

HAGN, H., 1972. Über kalkalpine paleozäne und untereozäne Gerölle aus dem bayerischen Alpenvorland. — Mitt. bayer. Staatssamml. Paläont. Hist. Geol., **12**:113–124, München.

HANZAWA, S., 1947. Note on an Eocene foraminiferal limestone from New Britain. — Jap. Jour. Geol. Geogr., **18**(4):59–61.

HINTE, J. E. van, 1963. Zur Stratigraphie und Mikropaläontologie der Oberkreide und des Eozäns des Krappfeldes (Kärnten). — Jb. Geol. B.-A., Sonderband **8**:1–147, Wien.

HOTTINGER, L., 1973. Selected Paleogene Larger Foraminifera. – [in:] HALLAM, A. (ed.). Atlas of Palaeobiogeography. — :443–452, Amsterdam – London – New York (Elsevier).

HOTTINGER, L., 1983. Neritic Macroid Genesis, an Ecological Approach. – [in:] PERYT, T. M. (ed.). Coated Grains. — :38–55, Berlin – Heidelberg (Springer).

HOTTINGER, L., HALICZ, E. & REISS, Z., 1993. Recent Foraminifera from the Gulf of Aquaba, Red Sea. — Dela SAZU, **33**:VI + 179 pp., Ljubljana.

HÖFLING, R. & MOUSSAVIAN, E., 1990. Paleocene acervulinid foraminifera – their role as encrusting, rhodolith-forming and reef-building organisms. — Abstr. 13th Int. Sedimentol. Congr.:227–228, Nottingham.

LITTLER, M. M., LITTLER, D. S. & HANISAK, M. D., 1991. Deep-water rhodolith distribution, productivity, and growth history at sites of formation and subsequent degradation. — J. Exp. Mar. Biol. Ecol., **150**:163–182.

LOGAN, B. W., HARDING, J. L., AHR, M., WILLIAMS, J. P. & SLEEP, R. G., 1969. Late Quaternary carbonate sediments of the Yucatan shelf, Mexico. – [in:] MCBIRNEY (ed.): Tectonic Relations of Northern Central America and the Western Caribbean – the Bonacca Expedition. — Mem. Amer. Assoc. Petrol. Geol., **11**:5–128, Tulsa.

LUTERBACHER, H. P., 1982. Zur Palökologie der Foraminiferen im Paleogen der Südpyrenäen. — N. Jb. Geol. Paläont. Abh., **164**:288–289, Stuttgart.

MANKER, J. P. & CARTER, B. D., 1987. Paleoecology and Paleogeography of an Extensive Rhodolith Facies from the Lower Oligocene of South Georgia and North Florida. — Palaios, **2**:181–188, Tulsa.

©Verein zur Förderung der Paläontologie am Institut für Paläontologie, Geozentrum Wien

MCGOWRAN, B., 1989. Silica burp in the Eocene ocean. — Geology, **17**:857–860, Boulder.

MINNERY, G. A., REZAK, R. & BRIGHT, T. J., 1985. Depth Zonation and Growth form of Crustose Coralline Algae: Flower Garden Banks, Northwestern Gulf of Mexico. – [in:] TOOMEY, D. F. & NITECKI, M. H. (eds.): Paleoalgology. — :237–247, Berlin – Heidelberg (Springer).

MOUSSAVIAN, E., 1984. Die Gosau- und Alttertiär-Gerölle der Angerberg-Schichten (Höheres Oligozän, Unterinntal, Nördliche Kalkalpen). — Facies, **10**:1–86, Erlangen.

MOUSSAVIAN, E., 1988. Die Peyssonneliaceen (auct.: Squamariaceae; Rhodophyceae) der Kreide und des Paläogen der Ostalpen. — Mitt. Bayer. Staatsslg. Paläont. hist. Geol., **28**:89–124, München.

MOUSSAVIAN, E. & HÖFLING, R., 1993. Taxonomische Position und Palökologie von *Solenomeris* DOUVILLE 1924 und ihre Beziehung zu *Acervulina* SCHULTZE, 1854 und *Gypsina* CARTER, 1877 (Acervulinidae, Foraminiferida). — Zitteliana, **20**: 263–276, München.

PENECKE, K. A., 1884. Das Eozän des Krappfeldes in Kärnten. — Sitzber. Österr. Akad. Wiss, math. naturw. Kl., Abt. I, **90**:327–371, Wien.

PERRIN, C., 1992. Signification ecologique des foraminiféres acervulinidés et leur rôle dans la formation de faciès récifaux et organogènes depuis le Paléocène. — Geobios, **25**(6):725–751, Lyon.

PERYT, T. M., 1983. Classification of Coated Grains. – [in:] PERYT, T. M. (ed): Coated grains. — :3–6, Berlin – Heidelberg (Springer).

PFENDER, J., 1936. Sur un organisme constructeur des calcairees crétacés et nummulitiques: *Pseudolithothamnium album* nov. gen. nov. sp. — Bull. Soc. Geol. France (5)**6**:303–308, Taf. 19, Paris.

PILLER, W. E. & P. PERVESLER, 1989. The Northern Bay of Safaga (Red Sea, Egypt): An Actuopalaeontological Approach. I. Topography and Bottom Facies. — Beitr. Paläont. Österr., **5**:103–147, Wien.

PLAZIAT, J. C. & PERRIN, C., 1992. Multikilometer-sized reefs built by foraminifera (*Solenomeris*) from the early Eocene of the Pyrenean domain (S. France, N. Spain): Palaeoecologic relations with coral reefs. — Palaeogeogr. Palaeoclimatol. Palaeoecol., **96**:195–231, Amsterdam.

PLUMLEY, W. J., RISLEY, G. A., GRAVES, R. W. & KALEY, M. E., 1962. Energy index for limestones interpretation and classification. — Mem. Amer. Ass. Petrol., Geol., **1**:85–107, Tulsa.

REID, R. P. & MACINTYRE, I. G., 1988. Foraminiferal-Algal Nodules from the Eastern Caribbean: Growth History and Implications on the Value of Nodules as Paleoenvironmental Indicators. — Palaios, **3**:424–435, Tulsa.

SCOFFIN, T. P., STODDART, D. R., TUDHOPE, A. W. & WOODROFFE, C., 1985. Rhodoliths and coralliths of Muri Lagoon, Rarotonga, Cook Islands. — Coral Reefs, **4**:71–80, Berlin – Heidelberg.

STENECK, R. S., 1985. Adaptions of Crustose Coralline Algae to Herbivory: Patterns in Space and Time. – [in:] TOOMEY, D. F. & NITECKI, M. H. (eds.): Paleoalgology. — :352–366, Berlin – Heidelberg (Springer).

TABERNER, C. & BOSENCE, D. W. J., 1985. Ecological Successions from Corals to Coralline Algae in Eocene Patch Reefs, Northern Spain. – [in:] TOOMEY, D. F. & NITECKI, M. H. (eds.): Paleoalgology. — :226–236, Berlin – Heidelberg (Springer).

TOLLMANN, A., 1977. Geologie von Österreich. Bd. **I**: Die Zentralalpen. — XVI + 766 S., Wien (Deuticke).

TOOMEY, D. F., 1975. Rhodoliths from the Upper Paleozoic of Kansas and the Recent – a comparison.— N. Jahrb. Geol. Paläont., Monatsh., **4**:242–255, Stuttgart.

TRAUTH, F., 1918. Das Eozänvorkommen bei Radstadt im Pongau und seine Beziehung zu den gleichaltrigen Ablagerungen bei Kirchberg am Wechsel und Wimpassing am Leithagebirge. — Denkschr. K. Akad. Wiss. Wien, math.-naturwiss. Kl., **95**:171–278, Wien.

TUCKER, M. E. & WRIGHT, V P., 1990. Carbonate sedimentology. — XII + 482 pp., Oxford – London (Blackwell).

WEBER VAN BOSSE, A. & FOSLIE, M., 1904. The corallinaceae of the Siboga – Expedition. – Siboga Exped. Monog., **41**, London.

WILKENS, E., 1989. Paläogene Sedimente des Krappfeldes und seiner Umgebung. — Arbeitstagung Geol. B.-A., **1989**:85–99, Wien.

WILKENS, E., 1991. Das zentralalpine Paläogen der Ostalpen: Stratigraphie, Sedimentologie und Mikrofazies Großforaminiferen reicher Sedimente. — Unpubl. Diss. Fachber. Geowiss. Univ. Hamburg:227 S., Hamburg.

WOELKERLING, W. J., 1988. The coralline red algae: an analysis of the genera and subfamilies of nongeniculate corallinaceae. — XI + 268 pp., London – Oxford (Oxford United Press).

WRAY, J. L., 1977. Calcareous Algae. — XIV + 185 pp., Amsterdam – Oxford – New York (Elsevier)

©Verein zur Förderung der Paläontologie am Institut für Paläontologie, Geozentrum Wien

PLATES 1 – 4

©Verein zur Förderung der Paläontologie am Institut für Paläontologie, Geozentrum Wien

PLATE 1
Facies

Fig. 1: *Pseudogypsina* Facies. Note the U-shaped growth form of *P. multiformis* TRAUTH, 1918 and their micrite envelopes. Dark particles are mostly coralline algal fragments (sample no. A24B).

Fig. 2: A weakly cemented portion of the *Pseudogypsina* Facies showing the growth form of *P. multiformis*.

Fig. 3: Rhodolith Facies with *Sphaerogypsina globulus* (REUSS, 1848) in the upper right part (sample no. A18B).

Fig. 4: Siliciclastic Coralline Algal Facies with a specimen of *Discocyclina* sp. and a bryozoan fragment in the lowermost part (sample no. C8).

Fig. 5: Siliciclastic *Pseudogypsina* Facies. Note the poorly sorted quartz grains (light colour) (sample no. C12).

Fig. 6: *Nummulites–Fabiania* Facies with *Nummulites* sp. and three different sections of *Fabiania cassis* (OPPENHEIM, 1896) (sample no. C15).

Fig. 7: *Alveolina–Orbitolites* Facies with an axial section of a large *Orbitolites* sp. indet. and several specimens of *Alveolina* div. spec. (sample no. H5).

Fig. 8: *Nummulites*–Rhodolith Facies. Nummulite tests are encrusted by coralline algae (sample no. UF1).

©Verein zur Förderung der Paläontologie am Institut für Paläontologie, Geozentrum Wien

PLATE 1

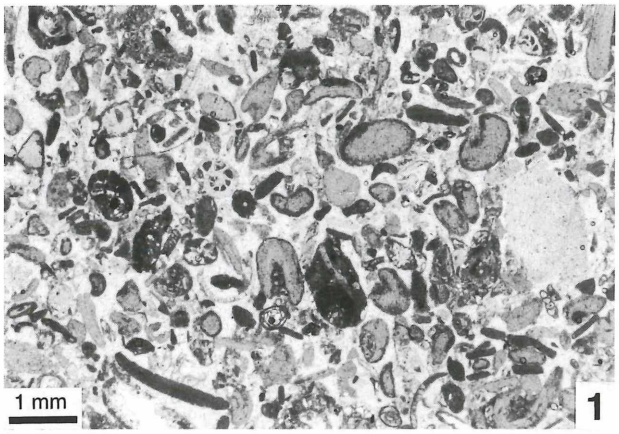

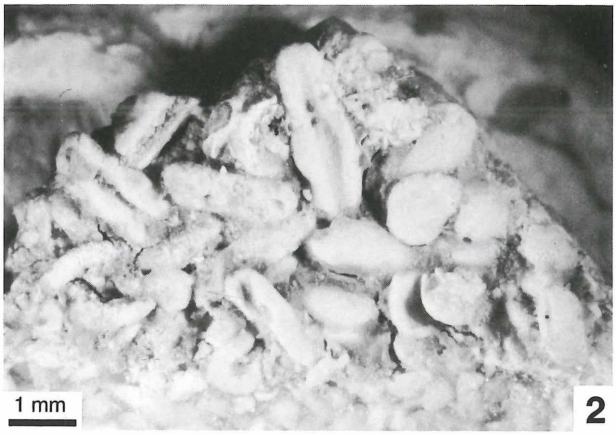

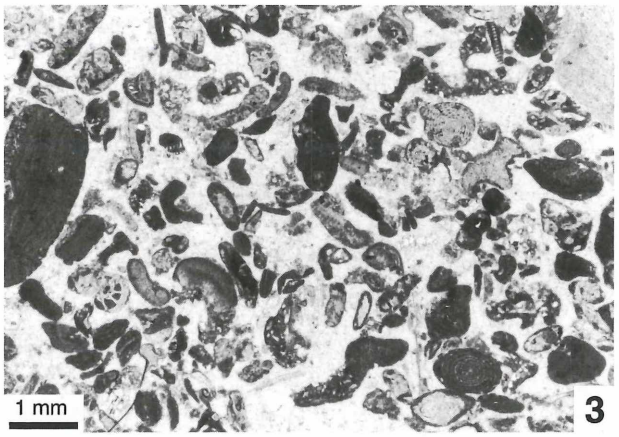

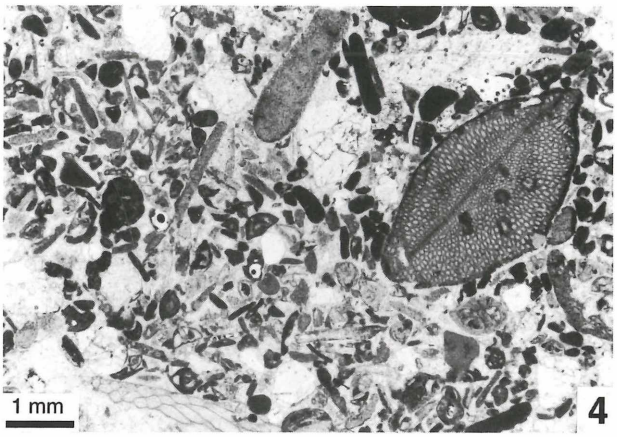

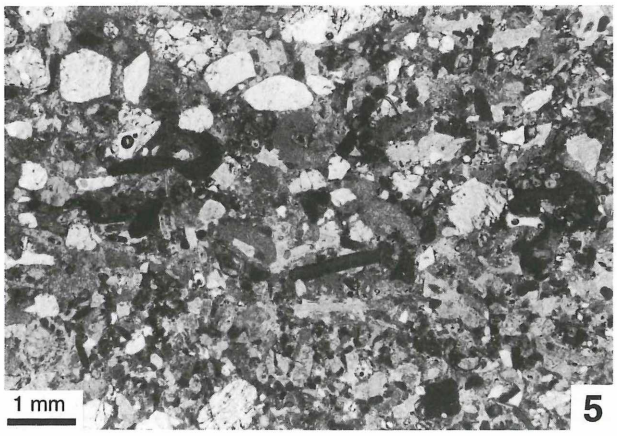

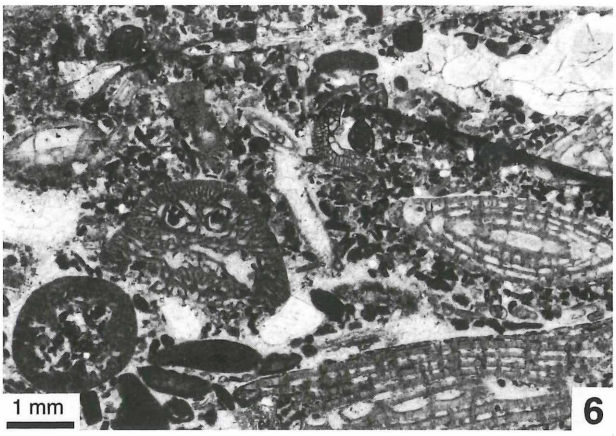

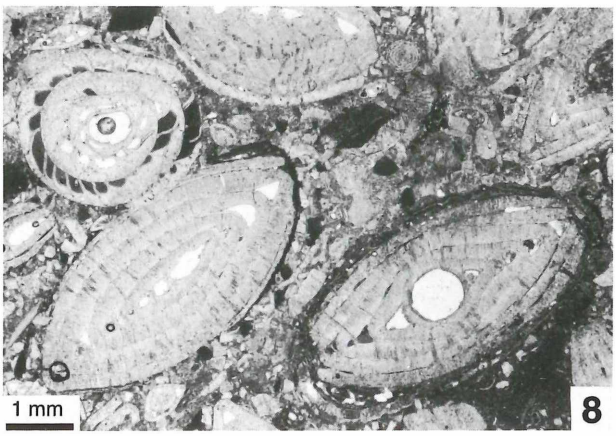

©Verein zur Förderung der Paläontologie am Institut für Paläontologie, Geozentrum Wien

PLATE 2

Growth forms

Fig. 1: Columnar rhodolith, predominantly consisting of *Sporolithon* sp. A. Nucleus not preserved. Lower Rhodolith Accumulation (sample no. UB3).

Fig. 2: Detail of Fig. 1, showing the final encrustation by *Acervulina ogormani* (DOUVILLE, 1924) (A), in competition with *Lithothamnion* sp. (L). Lower Rhodolith Accumulation (sample no. UB3).

Fig. 3: Dichotomously branched rhodolith, predominantly consisting of *Sporolithon* sp. A. Note the test of *Fabiania cassis* (OPPENHEIM, 1896) (arrow). Lower Rhodolith Accumulation (sample no. F2).

Fig. 4: Columnar growth form of *Sporolithon* sp. B, overgrown by *Pseudolithothamnium album* PFENDER, 1936. Lower Rhodolith Accumulation (sample no. U9–2A).

Fig. 5: Growth form of *Pseudolithothamnium album* PFENDER, 1936, intergrowing with *Acervulina ogormani* (A). On the right: *Haddonia heissigi* HAGN, 1968. Lower Rhodolith Accumulation (sample no. A18C).

Fig. 6: Columnar rhodolith with a coral nucleus. Formed predominantly by *Sporolithon* sp. A and partially by *Lithothamnion* (L). Note the large chambered *Haddonia heissigi* (H). The irregular shape of the rhodolith is partially induced by the shape of the nucleus. Lower Rhodolith Accumulation (see also Fig. 4, chart 9) (sample no. F3).

Fig. 7: Rhodolith with a *Nummulites* nucleus, largely consisting of *Sporolithon* sp. A (see also Fig. 4, chart 1). Upper Rhodolith Accumulation (sample no. UF1).

Fig. 8: Laminar macroid of *Acervulina ogormani* (DOUVILLE, 1924) with a coral nucleus. Macroid horizon (sample no. U26).

Fig. 9: Part of a columnar *Acervulina ogormani* - macroid; compare Fig. 5. Note the intergrown homotrematid foraminifera (arrows). Macroid horizon (sample no. H9–5B).

©Verein zur Förderung der Paläontologie am Institut für Paläontologie, Geozentrum Wien

PLATE 2

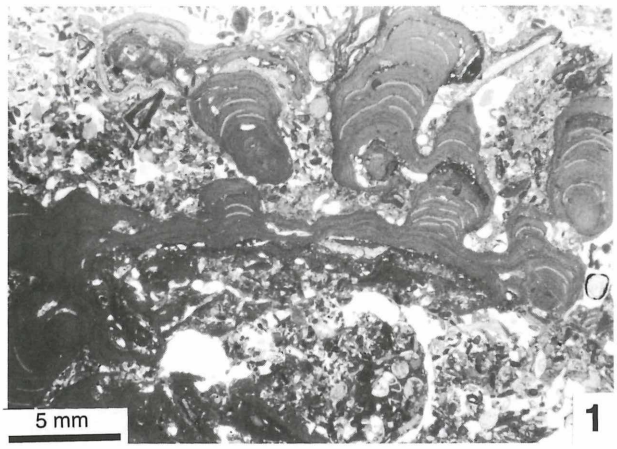

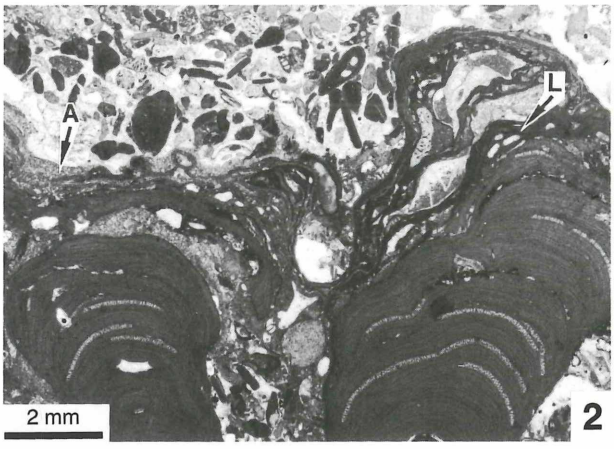

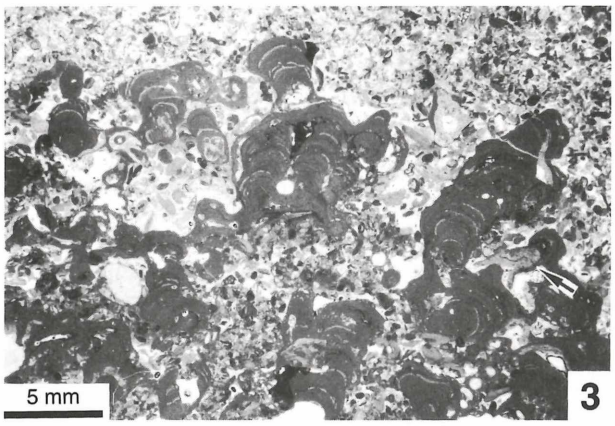

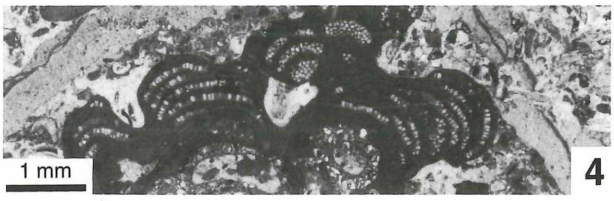

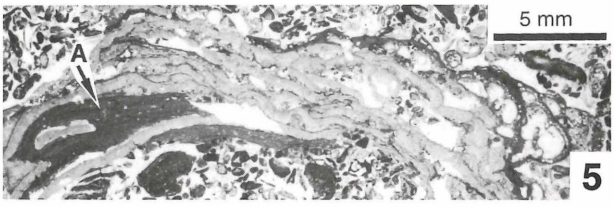

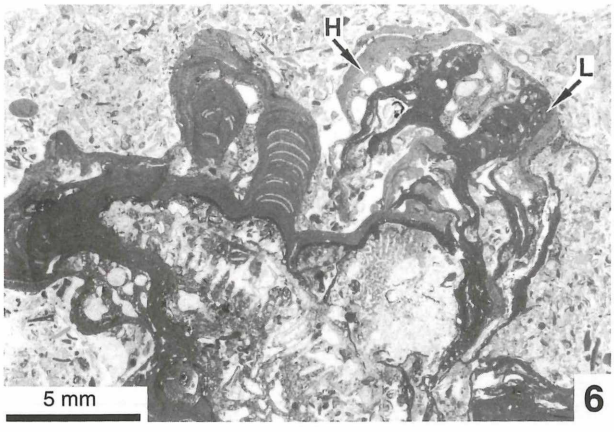

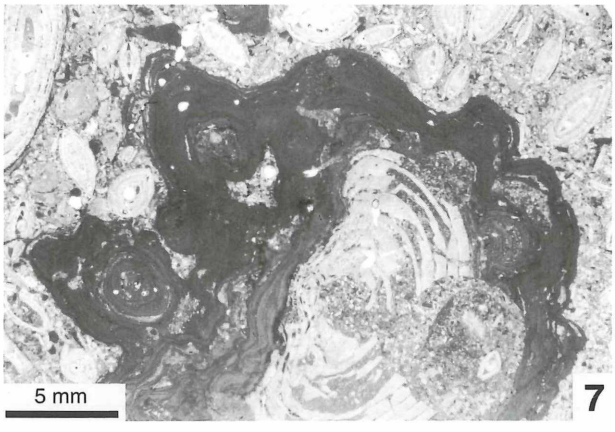

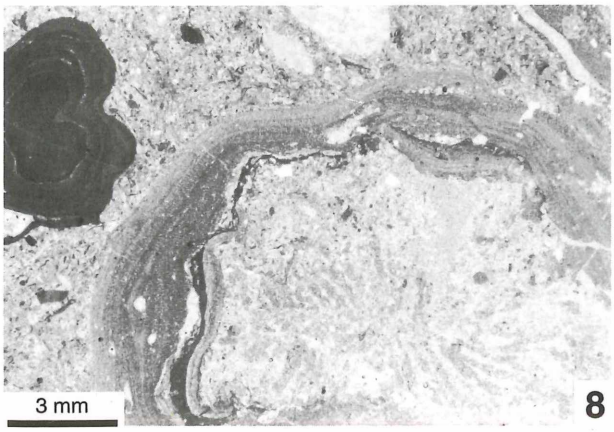

©Verein zur Förderung der Paläontologie am Institut für Paläontologie, Geozentrum Wien

PLATE 3

Taxonomy – Rhodophyceae

Fig. 1: *Sporolithon* sp. A, showing the characteristic regular rows of conceptacles and poorly developed core filaments ("Hypothallus"; arrow) (sample no. UB3).

Fig. 2: *Sporolithon* sp. B. Note shape and size of conceptacles, contrasting to *S.* sp. A (sample no. U9–2A).

Fig. 3: *Lithoporella melobesioides* (FOSLIE) FOSLIE, 1909, overgrowing *Acervulina ogormani* (DOUVILLE, 1924) (sample no. H9–3B).

Figs. 4, 5: *Lithothamnion* sp. Fig. 4 shows the characteristic conceptacle, Fig. 5 the core filaments characteristically differing from those of *Sporolithon* (Fig. 1) (sample no. F3).

Fig. 6: *Pseudolithothamnium album* showing characteristic consecutive tiers (sample no. A18C).

Fig. 7: Detail of Fig. 6. Note the median cell layer and outward curving filaments.

©Verein zur Förderung der Paläontologie am Institut für Paläontologie, Geozentrum Wien

PLATE 3

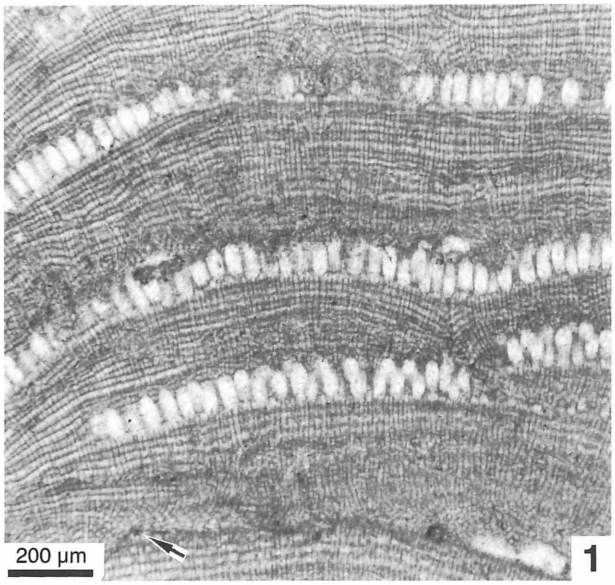

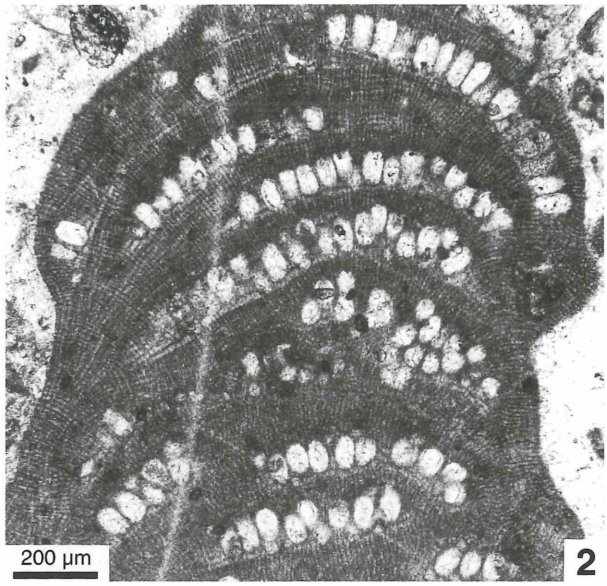

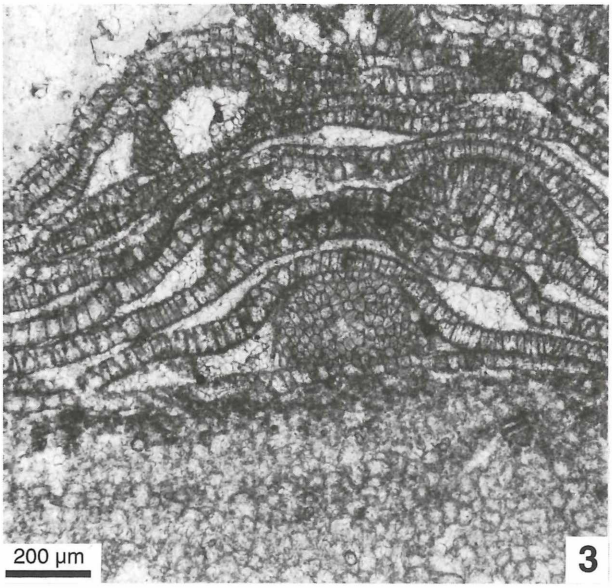

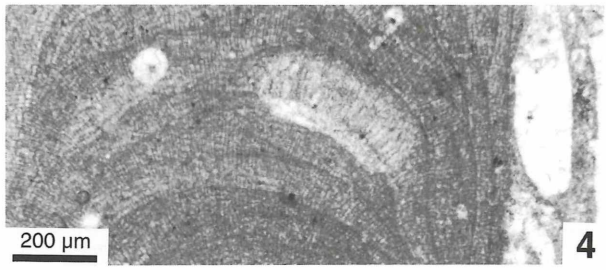

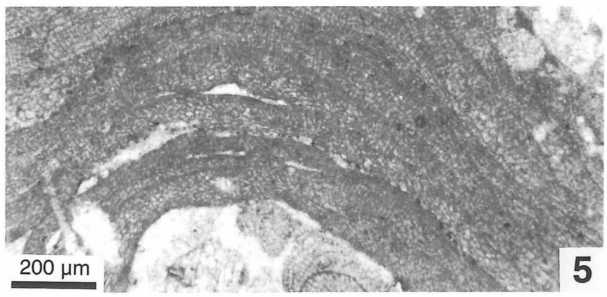

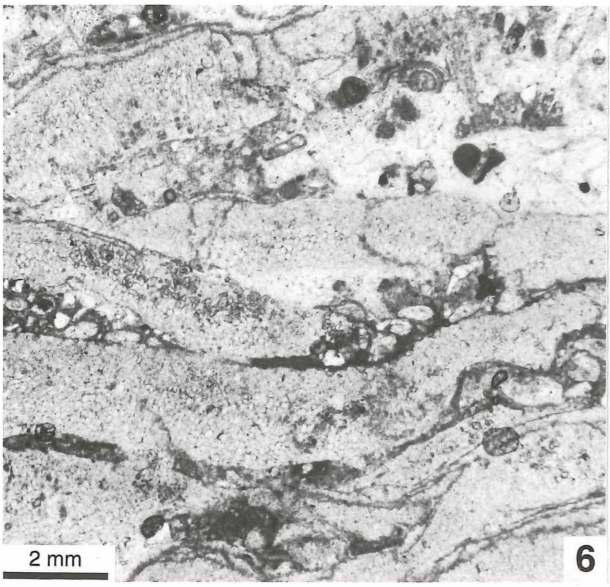

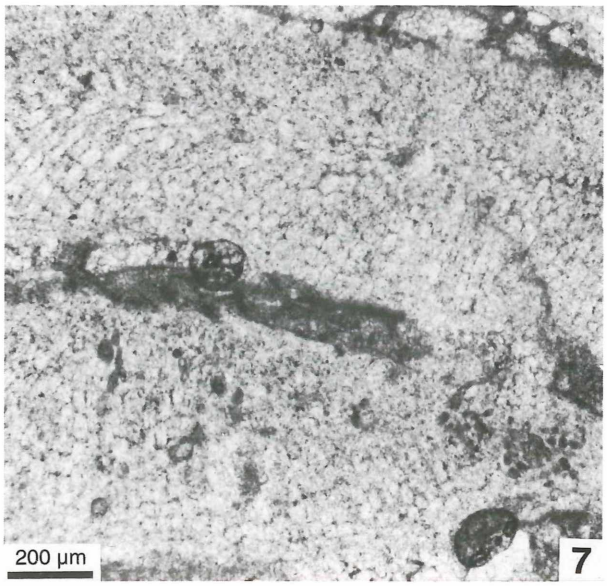

©Verein zur Förderung der Paläontologie am Institut für Paläontologie, Geozentrum Wien

PLATE 4

Taxonomy – Foraminifera

Fig. 1: Juvenarium of *Acervulina ogormani* (DOUVILLE, 1924) and cells of encrusting stage (sample no. H9–5B).

Fig. 2: Juvenarium of *Acervulina linearis* HANZAWA, 1947, overgrowing a coralline alga (sample no. A11D).

Fig. 3: Characteristic borings in rhodoliths. The shape (smooth-walled, sinuous boring with a rounded blind end) corresponds with sipunculid borings (BOSENCE, 1984) (sample no. U24).

Fig. 4: *Haddonia heissigi* HAGN, 1968. Note the intercalations of coralline algae (dark layers) (sample no. A18C).

Fig. 5: Detail of Fig. 4. Chambers of *H. heissigi*. Note the inner hyaline layer (arrow) characteristic for this genus and intergrowings of *Lithoporella melobesioides* (L).

Fig. 6. Two layers of homotrematid foraminifera (large chambers), intergrowing with *Acervulina ogormani* (sample no. H9–5B).

Fig. 7. Serpulid worm tube in an acervulinid macroid (sample no. H9–5B).

©Verein zur Förderung der Paläontologie am Institut für Paläontologie, Geozentrum Wien

PLATE 4

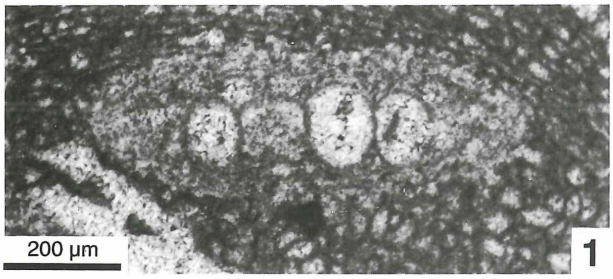

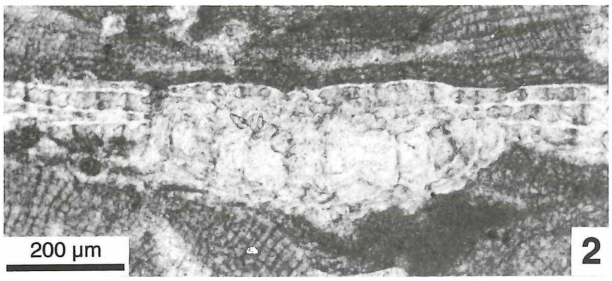

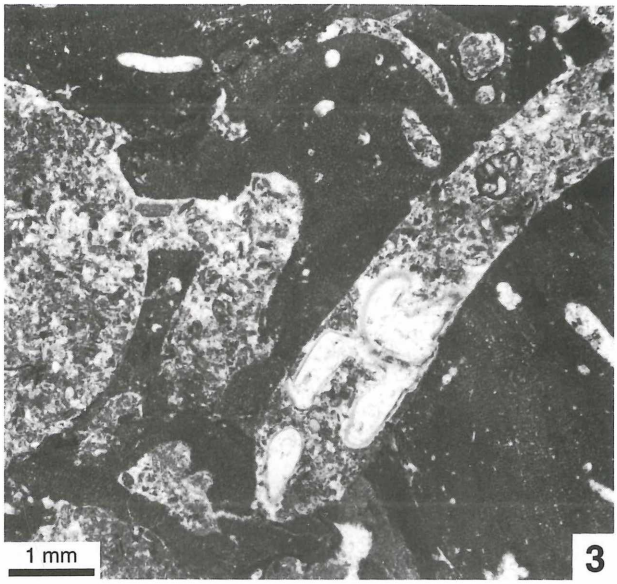

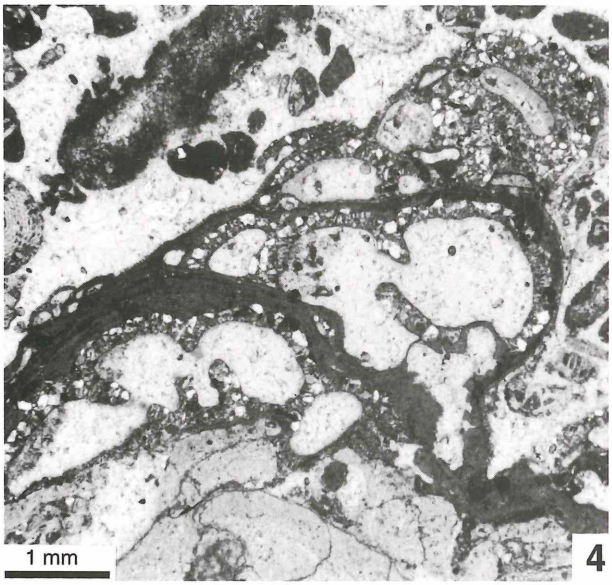

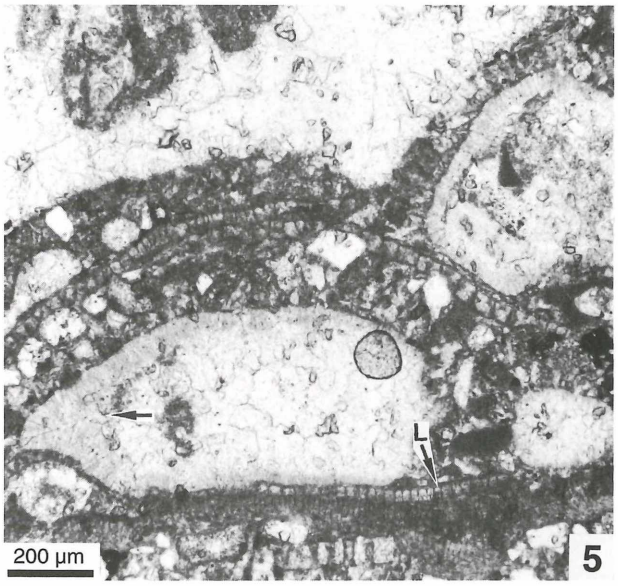

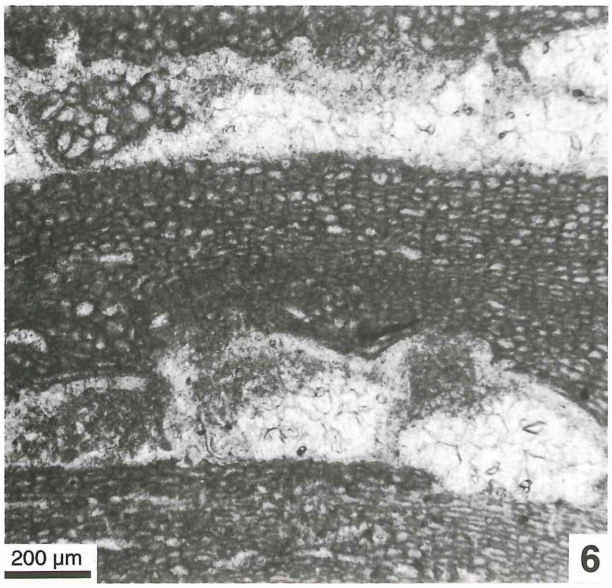

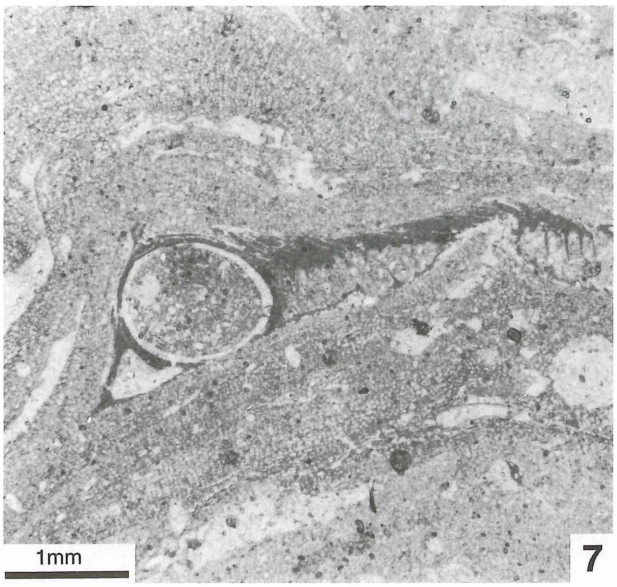

ZOBODAT - www.zobodat.at

Zoologisch-Botanische Datenbank/Zoological-Botanical Database

Digitale Literatur/Digital Literature

Zeitschrift/Journal: Beiträge zur Paläontologie

Jahr/Year: 1994

Band/Volume: 19

Autor(en)/Author(s): Rasser M

Artikel/Article: Facies and palaeoecology of rhodoliths and acervulinid macroids in the Eocene of the Krappfeld (Austria) 191-217